**Atmospheric
Chemistry
and Physics**

Functionalization and fragmentation during ambient organic aerosol aging: application of the 2-D volatility basis set to field studies

B. N. Murphy[1], N. M. Donahue[1], C. Fountoukis[2], M. Dall'Osto[3,4], C. O'Dowd[4], A. Kiendler-Scharr[5], and S. N. Pandis[1,6]

[1]Department of Chemical Engineering, Carnegie Mellon University, 5000 Forbes Ave, Pittsburgh, Pennsylvania 15213, USA
[2]Institute of Chemical Engineering Sciences (ICEHT), Foundation for Research and Technology Hellas (FORTH), Patras, Greece
[3]National Center for Atmospheric Science, Division of Environmental Health and Risk Management, School of Geography, Earth & Environmental Sciences University of Birmingham Edgbaston, Birmingham B15 2TT, UK
[4]School of Physics and Centre for Climate and Air Pollution Studies, National University of Ireland Galway, Galway, Ireland
[5]IEK-8II: Troposphere, Forschungszentrum Jülich, Jülich, Germany
[6]Department of Chemical Engineering, University of Patras, Patra, Greece

Correspondence to: S. N. Pandis (spyros@andrew.cmu.edu)

Abstract. Multigenerational oxidation chemistry of atmospheric organic compounds and its effects on aerosol loadings and chemical composition is investigated by implementing the Two-Dimensional Volatility Basis Set (2-D-VBS) in a Lagrangian host chemical transport model. Three model formulations were chosen to explore the complex interactions between functionalization and fragmentation processes during gas-phase oxidation of organic compounds by the hydroxyl radical. The base case model employs a conservative transformation by assuming a reduction of one order of magnitude in effective saturation concentration and an increase of oxygen content by one or two oxygen atoms per oxidation generation. A second scheme simulates functionalization in more detail using group contribution theory to estimate the effects of oxygen addition to the carbon backbone on the compound volatility. Finally, a fragmentation scheme is added to the detailed functionalization scheme to create a functionalization-fragmentation parameterization. Two condensed-phase chemistry pathways are also implemented as additional sensitivity tests to simulate (1) heterogeneous oxidation via OH uptake to the particle-phase and (2) aqueous-phase chemistry of glyoxal and methylglyoxal.

The model is applied to summer and winter periods at three sites where observations of organic aerosol (OA) mass and O:C were obtained during the European Integrated Project on Aerosol Cloud Climate and Air Quality Interactions (EUCAARI) campaigns. The base case model reproduces observed mass concentrations and O:C well, with fractional errors (FE) lower than 55 % and 25 %, respectively. The detailed functionalization scheme tends to overpredict OA concentrations, especially in the summertime, and also underpredicts O:C by approximately a factor of 2. The detailed functionalization model with fragmentation agrees well with the observations for OA concentration, but still underpredicts O:C. Both heterogeneous oxidation and aqueous-phase processing have small effects on OA levels but heterogeneous oxidation, as implemented here, does enhance O:C by about 0.1. The different schemes result in very different fractional attribution for OA between anthropogenic and biogenic sources.

1   Introduction

Atmospheric fine particulate mass (PM$_{2.5}$) has been implicated in increased mortality and morbidity rates in human populations (Pope et al., 2009) and it represents an uncertain link between anthropogenic activities and global climate forcing (IPCC, 2007; Isaksen et al., 2009). Although associations between the specific chemical composition of these particles and their health and climate effects are complex and remain uncertain, a significant fraction (20–90 %) of fine particulate mass is directly attributable to organic compounds (Zhang et al., 2007; Morgan et al., 2010b). A thorough understanding of the formation pathways and atmospheric evolution of these gas- and aerosol-phase compounds is necessary in order to understand the atmospheric particle system as a whole.

The atmospheric organic aerosol (OA) system is complex. OA consists of thousands of individual compounds (Goldstein and Galbally, 2007), each with their own characteristic emission sources, volatilities, chemical reactivity with regard to the hydroxyl radical and other atmospheric oxidants and degradation pathways (Atkinson and Arey, 2003; Kanakidou et al., 2005; Kroll and Seinfeld, 2008; Hallquist et al., 2009). It has long been known that oxidation of volatile organic compounds (VOC) can lead to production of semivolatile species that readily partition to the particle phase (Grosjean and Seinfeld, 1989; Pandis et al., 1992; Odum et al., 1997; Griffin et al., 1999). However, our understanding is based on laboratory observations made over timescales on the order of hours to a day, but atmospheric particles are typically airborne for about a week (Pandis et al., 1995), and are continually exposed to oxidants until they are removed. This continued oxidation (aging) is a complex process with uncertain impacts.

Efforts to describe the evolution of OA mass concentration over time in computational models have followed two general approaches recently: (1) explicit simulation of the emission, gas/particle partitioning and deposition of specific identifiable chemical species (Griffin et al., 2002; Pun et al., 2002; Johnson et al., 2006) or (2) treatment of species relevant to organic aerosol formation via classes of compounds lumped by similarities in some intensive property such as volatility, carbon number, oxidation state, or polarity (Donahue et al., 2006, 2011; Pankow and Barsanti, 2009). The first approach may eventually be able to explain OA formation and aging based on first principles (Aumont et al., 2005). However, the current uncertainty about the physical properties of many of these species (e.g. vapor pressure, activity coefficients) and the corresponding rates of the various chemical pathways introduce substantial uncertainties in the results of this approach. In addition the computational burden of explicitly modeling the atmospheric transport and fate of thousands of species makes implementation of this explicit approach in a regional- or global-scale chemical transport model (CTM) extremely challenging. The sec-

ond approach exploits the highly "averaged" nature of the real atmosphere and tries to describe the initial oxidation and subsequent aging processes as they act on primary organic compounds. Treating the OA system as a conceptually simplified mixture of surrogate chemical species is advantageous when predicting the OA concentration and properties in a large-scale CTM.

The equilibrium gas/particle partitioning calculations used in most current OA models are based on the assumption that the corresponding organic compounds reach equilibrium in the atmosphere in timescales of minutes or tens of minutes. Vaden et al. (2011) challenged that assumption when they measured evaporation rates for α-pinene-generated SOA to be much slower than expected. However, the interpretation of these results depends on both the definition of equilibration timescale (i.e. evaporation time is not the same as equilibration time) and the experimental concentrations chosen. Stanier et al. (2007) gently heated α-pinene SOA in a smog chamber and found that it evaporated and equilibrated in minutes. Lee et al. (2011) heated SOA from α-pinene, β-pinene, and limonene in a thermodenuder. That study found that evaporation could be modeled with the existing VBS parameterization and modest mass transfer delays. When the residence time was extended to approximately one minute particle sizes reached those predicted by equilibrium calculations.

The two-dimensional volatility basis set (2-D-VBS) tracks volatility (as effective saturation mass concentration, C^*, in $\mu g\,m^{-3}$) and oxidation state (as ratio of elemental oxygen to carbon, O:C) of a population of organic compounds (Jimenez et al., 2009). The scheme directly uses effective saturation concentration to predict OA mass concentration after gas-particle equilibrium is achieved through an absorptive partitioning process. The O:C dimension allows comparison of model predictions with aerosol mass spectrometer (AMS) measurements to evaluate our conceptual model of atmospheric organic aerosol aging. O:C is a useful metric for analyzing OA aging in that species generally increase in O:C with every oxidation reaction (Kroll et al., 2011; Murphy et al., 2011). Volatility, on the other hand, should change to some degree with every oxidation step but may increase or decrease with complex dependencies on the nature of the reaction mechanism. A key is the relative role of functionalization processes, which tend to decrease volatility, and fragmentation of C-C bonds, which tends to increase volatility (Jimenez et al., 2009; Kroll et al., 2009; Chacon-Madrid et al., 2010). The complicated interactions between functionalizing and fragmenting pathways and the rates at which they occur in both the vapor and aerosol phases will likely influence source-receptor relationships. Unfortunately, isolating these processes in smog-chamber experiments is an exceedingly difficult task. We argue that a CTM employing the 2-D-VBS combined with the corresponding field measurements is well-suited to probe the sensitivity of modeled atmospheric OA formation to various aging schemes and assess

the reasonableness with which those schemes represent both ambient OA loadings and chemical composition.

The 2-D-VBS scheme has been evaluated for one measurement site from the EUCAARI summer campaign (Murphy et al., 2011). That study used a Lagrangian CTM to model one-dimensional columns of air as they approached Finokalia, a remote location on the island of Crete in Greece. The base-case OA aging model assumed that the products from each OH aging reaction have an effective saturation concentration one order of magnitude lower than the reactant. This scheme is a simple parameterization of the effects of aging on organic compounds that was based on laboratory and CTM studies (Robinson et al., 2007; Lane et al., 2008; Grieshop et al., 2009; Murphy and Pandis, 2009). The model performed reasonably well in predicting OA mass (predicted average of $3.3 \, \mu g \, m^{-3}$ fell close to measured average of $3.1 \, \mu g \, m^{-3}$) and O:C (diurnally-averaged predictions fell within 20 % of measurements) for the Finokalia summer study. Several sensitivity tests were also performed, all based on the fundamental assumption that organic compounds only functionalized when oxidized. Those tests revealed that continually reducing the volatility of both anthropogenic and biogenic OA compounds (assuming a reasonable reaction rate constant with the hydroxyl radical, $k_{OH} = 1 \times 10^{-11} \, cm^3$ $molec^{-1} \, s^{-1}$) would overpredict the OA measured at Finokalia; similar conclusions have been reached with 3-D CTMs (Lane et al., 2008; Murphy and Pandis, 2010) and confirmed by smog chamber results (Donahue et al., 2012b). Those studies interpreted this overprediction in rural areas as a possible indication that multigenerational aging results in a net average decrease in volatility for anthropogenic SOA but no net average change in volatility for biogenic SOA, presumably due to a balancing of fragmentation and functionalization effects. Bergström et al. (2012) modeled carbonaceous aerosols across Europe for multiple seasons and years, experimenting with four different configurations of the VBS module. By comparing models with and without anthropogenic and biogenic aging effects, they concluded that the assumptions regarding aging have significant consequences for the fraction of total OA mass that the model predicts to be attributed to anthropogenic or biogenic sources. The current study, by explicitly including detailed functionalization and fragmentation of SOA from all sources, takes a rigorous look at this assumption.

Understanding has grown significantly in the last decade of both condensed-phase chemistry involving hydroxyl radical reactive uptake to OA containing particles (Rudich et al., 2007) as well as aqueous-phase processing of species like glyoxal and methylglyoxal (Carlton et al., 2008; Sareen et al., 2010; Ervens et al., 2011). However, these processes are still regarded as highly uncertain contributors to atmospheric OA chemistry (Fuzzi et al., 2006; Hallquist et al., 2009). Aqueous-phase chemistry may enhance O:C or OA mass significantly if it can produce low volatility compounds with high oxygen content. The base-case mechanism

is constrained by smog-chamber studies which, for the most part, have found it difficult to reproduce O:C values as high as ambient measurements (Chhabra et al., 2010; Ng et al., 2010; Qi et al., 2010). Recently, Chen et al. (2011) produced SOA from isoprene with higher O:C (0.75–0.88) but results with α-pinene and β-caryophyllene SOA were much lower (0.33–0.52 and 0.33–0.54, respectively). Those authors hypothesized that particle-phase reactions close the gap between chemical composition measured in the lab and that observed in the field. Here we implement reasonable approximations to condensed-phase processes and analyze their impacts on model-predicted OA mass concentrations and O:C over relevant atmospheric timescales.

Building on the Murphy et al. (2011) framework, we extend the analysis in the current study to include two more measurement sites with good AMS datasets (Mace Head, Ireland and Cabauw, Netherlands), and explore model behavior for a winter period (February/March 2009). Further, we introduce more detailed functionalization and fragmentation schemes to the model and assess them at these particular sites. Finally, we examine the impact on model predictions of both OA concentration and O:C when other proposed OA formation pathways (heterogeneous hydroxyl uptake and aqueous-phase processing) are incorporated in the model framework.

2 Application to the EUCAARI campaigns

2.1 Measurements

One of the major objectives of the EUCAARI campaigns was quantification of the relationship between anthropogenic aerosol particles and regional air quality (Kulmala et al., 2009). Several AMS instruments were deployed to sites throughout Europe in May 2008 and February/March 2009 during EUCAARI intensives (Kulmala et al., 2011). This study will focus on observations made at two remote sites (Finokalia, Greece and Mace Head, Ireland) and one suburban site (Cabauw, Netherlands). In this way, the model will be evaluated not only under a variety of meteorological and photochemical conditions, but also under a variety of source influences.

Summertime observations at Finokalia were conducted from 8 May to 4 June 2008 (Pikridas et al., 2010). The solar radiation was intense during the period, with daily maxima always exceeding $850 \, W \, m^{-2}$. The non-refractory PM_1 chemical composition was measured with an Aerodyne quadrupole aerosol mass spectrometer (Q-AMS) as described in detail by Hildebrandt et al. (2010a). Using the organic mass at $m/z \, 44$ as measured by the Q-AMS, they estimated O:C with the parameterization of Aiken et al. (2008). The contribution from $m/z \, 57$ (characteristic of fresh, hydrocarbon-like organic species) was barely detectable throughout the campaign, indicating that heavily

aged organic aerosol was arriving at the site regardless of the source location. The winter campaign at Finokalia took place from 25 February to 25 March 2009 and the OA was much less oxidized than in the summer (average O:C = 0.5 and 0.8, respectively) as documented by Hildebrandt et al. (2010b). That study also found the OA chemical composition to be much more variable in the winter than the summer and concluded that decreases in photochemical activity in the wintertime likely explain the discrepancy. Here we have chosen 9 summer days and 10 winter days for evaluation because these days were characterized by air parcels originating from Europe within the previous 48 h instead of originating from Africa or from western parts of the Mediterranean Sea, where emission inventories are more uncertain.

The Mace Head Atmospheric Research Station is influenced by air masses that range from exceedingly clean (those that arrive directly from the west) to polluted continental outflow (Dall'Osto et al., 2010). Here, a High Resolution Time of Flight Aerosol Mass Spectrometer (HR-ToF-AMS) was deployed from 16 May to 13 June 2008 and 26 February to 26 March 2009. O:C values were calculated explicitly rather than estimated from the m/z 44 results. Parcel trajectories arriving from the European continent tended to correlate with warm, sunny conditions, leading to higher degrees of oxidation. We focus on periods when polluted air masses arrived at the site from Europe, selecting 7 summer days and 5 winter days.

The model must be able to capture near-source OA formation and processing in addition to longer-range regional transport and aging. The Cabauw station is located in a rural, agricultural area of the Netherlands; however, it is close to large urban sources (about 30 km from Rotterdam and Utrecht, 50 km from Amsterdam). Organic aerosol concentrations were observed with a HR-ToF-AMS from 28 April to 30 May 2008 and 25 February to 25 March 2009. The spring dates were characterized by regional pollution events with high contribution of organics to PM$_1$ (Morgan et al., 2010a), whereas in winter nitrate was the dominant component (Mensah et al., 2012). Dates from these sets were selected for model comparison in order to avoid regional stagnation events that would make simulation with a one-dimensional Lagrangian transport model exceedingly difficult. This selection criterion still includes parcels that have arrived from nearby countries east or southeast of the Netherlands. Eight summer and 10 winter days were chosen.

2.2 Chemical transport model

The CTM host model used in the current study was described in detail by Murphy et al. (2011). Briefly, the model simulates a one-dimensional column of air as it is advected through the European continental domain by wind fields obtained from the Weather Research and Forecast (WRF) model (Skamarock et al., 2008). The 10 grid-cell vertical column reaches 2.5 km in the atmosphere, with the first cell ris-

ing from the surface to 60 m height. The model takes into account atmospheric transport and chemical processes, including hourly emissions (both anthropogenic and biogenic), dry and wet deposition of gases and aerosols, gas-phase chemistry (SAPRC-99) and vertical turbulent dispersion. WRF is used offline to calculate the hourly gridded meteorological parameters (vertical dispersion coefficients, temperature, pressure, water vapor, clouds, and rainfall) that are used as inputs to the CTM.

Both wet and dry deposition are accounted for by the model. Dry deposition is a function of meteorological parameters and land use (not as important for particulate mass), while wet deposition is calculated from the precipitable water input from the WRF simulations. Since black carbon and sulfate are reproduced well by this model, it is fair to assume deposition of OA is treated reasonably. However, scavenging of organic gases is an uncertainty. Here, we assume all organic gases have an effective Henry's Law constant of 2700 M atm^{-1}. The sensitivity of mass predictions to this assumption has been explored in previous studies, but is still quite uncertain. Anthropogenic and biogenic emissions are input as hourly gridded fields. Anthropogenic gases include land emissions from the GEMS dataset (Visschedijk et al., 2007) and emissions from international shipping activities. Anthropogenic particulate matter mass emissions of organic and elemental carbon are based on the Pan-European Carbonaceous Aerosol Inventory (Denier van der Gon et al., 2009) that has been developed as part of the EUCAARI activities (Kulmala et al., 2009, 2011). Three different datasets are combined in order to produce the biogenic gridded emissions for the model. Emissions from ecosystems are produced offline by the Model of Emissions of Gases and Aerosols from Nature (MEGAN) (Guenther et al., 2006). Since sea surface covers a considerable portion of the domain, the marine aerosol model developed by O'Dowd et al. (2008) has been used with the submicron aerosol sea-spray source function from Geever et al. (2005) to estimate mass fluxes for both accumulation and coarse mode including the organic aerosol fraction. Wind speed data from WRF and chlorophyll a concentrations are the inputs needed for the marine aerosol model. Chlorophyll a data were acquired using the GES-DISC Interactive Online Visualization And aNalysis Infrastructure (GIOVANNI), part of NASA's Goddard Earth Sciences (GES) Data and Information Services Center (DISC). Wildfire emissions were also included (Sofiev et al., 2008a, b). The predictive capability of organic aerosol models is affected by uncertainties in these emissions inventories. Especially uncertain are the biogenic VOC inventories from MEGAN and the wood-burning inventories as pointed out by Simpson et al. (2007), possibly leading to well more than a factor of 2 uncertainty in the model's final OA mass prediction. However, the focus of this work is on uncertainty arising from the aging mechanism itself. Regardless of the magnitude of emissions from various sources, compounds begin their atmospheric residence time relatively reduced.

Thus any inability of the model to capture moderately high O:C when fragmentation is introduced is likely a result of inaccurately modeling a chemical process as opposed to an emission factor.

The CTM, its simulated processes, and associated input fields are based on a 3-dimensional implementation, PMCAMx-2008. Fountoukis et al. (2011) evaluated this larger model against ambient measurements at ground sites (Cabauw, Finokalia, Mace Head and Melpitz) and aboard aircraft for organic aerosol as well as inorganic aerosol components. That study found fractional errors at or less than 50 % and 30 % for sulfate and organic aerosol at all four sites. For all of the data combined, 70 % of the sulfate predictions and 87 % of the OA predictions were within a factor of 2 of the measurement. Fractional errors of 60 % were found for both species on board aircraft with 62 % of sulfate and 66 % of OA predictions within a factor of two of the altitude-dependent observations.

The Hybrid Single Particle Lagrangian Integrated Trajectory (HYSPLIT) model (Draxler et al., 2009) is used to calculate 72 back trajectories for each arriving air parcel. For consistency, this study uses the same meteorological fields (calculated by WRF) as input to HYSPLIT to calculate the back trajectories. To help mitigate uncertainty from wind shear, 20 trajectories are calculated for each arrival time by varying the height of the arriving parcel from ground level to the 2.5 km model ceiling. The HYSPLIT clustering analysis utility is then used to estimate the path of one trajectory that best represents the origins of the 20 sample trajectories simultaneously. PMCAMx-2008 includes an additional OA model species that is advected from outside the regional model boundaries. This species, background OA (bgOA), is assumed to be highly aged with very low volatility, and will be shown to be a minor influence on total OA mass concentrations at all of the sites for the model evaluation days chosen. The model is susceptible to certain weaknesses though, in particular its inability to realistically account for horizontal dispersion processes. This feature may lead to errors in overprediction (artificial build-up of pollutants) and underprediction (unaccounted for mixing of pollutants from sources not directly in the parcel's path). For this reason, this study will focus on analysis of averaged diurnal profiles of OA concentration and O:C instead of comparisons to hourly measurements, which is the focus of Fountoukis et al. (2011). In general, the performance of this 1-D model is similar but slightly worse than that of the full 3-D model. For instance, for Cabauw in the summer, the average measured sulfate was $1.5\,\mu g\,m^{-3}$ compared to $2.2\,\mu g\,m^{-3}$ for the 3-D model and $2.7\,\mu g\,m^{-3}$ for the 1-D model. The opposite trend is seen when comparing predicted NO_2 mixing ratios with observations at Cabauw. The trajectory model underpredicts NO_2 mixing ratios at Cabauw in the summer (observed average around 8 ppb) with an average bias of -2.3 ppb and root-mean-square error of 3.4 ppb. In winter, when observed mixing ratios are higher (average around 13 ppb), the model re-

sponds with increased concentrations and accuracy. The average bias for the winter simulations is -2.6 ppb. Along with this feature, a comparison of the corresponding fractional biases (0.06 for winter and 0.30 for summer) indicates that the one-dimensional model used is able to capture the average change in vertical dispersion with weather changes.

When performing the back-trajectory calculations, some air masses cross the western edge of the PMCAMx European domain and thus no input data is available to characterize their origin before that time. They may have originated further west, which presumably would allow the use of the 3-D model boundary conditions, assuming enough time passes before the parcel arrives at the observation site. However, it is also possible that these trajectories turned from the south, for instance, just past the western boundary and actually originated from the European continent. There is not enough information to constrain this so these days are not used in the simulations.

3 Organic aerosol aging

The OA module used for this study is based on the 2-D-VBS framework described in Donahue et al. (2011, 2012a). Organic aerosol mass is segregated into 12 bins along an axis of effective saturation concentration ($C^* = 10^{-5}$ to $10^6\,\mu g\,m^{-3}$ at 300 K) separated by an order of magnitude. This range includes intermediate volatility and semivolatile compounds important for atmospheric OA formation as well as low- and very low-volatility compounds that are important for comparisons to thermodenuder observations. Each C^* interval contains 13 bins to describe O:C (0.0 to 1.2 incremented by 0.1), so the complete 2-D-VBS for a given source class contains 156 bins.

Five OA source classes are resolved: (1) aSOA formed from the oxidation of anthropogenic VOCs, (2) bSOA formed from oxidation of biogenic VOCs, (3) POA species emitted with $C^* \leq 1000\,\mu g\,m^{-3}$, which may evaporate and recondense during atmospheric transport, (4) OH oxidation products of the semivolatile primary emissions, known as semi-volatile SOA (sSOA), and, (5) intermediate volatility SOA (iSOA) from primary emissions with $C^* > 1000\,\mu g\,m^{-3}$. We parameterize emissions of these intermediate volatility organic compounds (IVOCs) with the often-used 1.5 times the original POA mass emission rate (Robinson et al., 2007; Murphy and Pandis, 2009; Hodzic et al., 2010; Tsimpidi et al., 2010). This mass is susceptible to homogeneous oxidation by OH and may go to lower volatility and condense to form SOA.

For first-generation SOA yields from anthropogenic and biogenic VOCs, we use parameters that have been applied to the eastern US, Mexico City and EUCAARI domains with reasonable success (Murphy and Pandis, 2010; Tsimpidi et al., 2010; Fountoukis et al., 2011). In previous work, these first-generation products were assumed to have a uniform

O:C of 0.4 in the base case, but an alternative parameterization was considered with O:C varying with the saturation concentration of the product (Murphy et al., 2011). Given that the trend of increasing O:C with decreasing volatility has been confirmed in several laboratory and field studies (Huffman et al., 2009; Kostenidou et al., 2009; Shilling et al., 2009; Ng et al., 2010; Chen et al., 2011), this work will assume the latter, variable parameterization for first-generation SOA for all cases.

3.1   Base-case functionalization scheme

The primary focus of this work is to explore a variety of proposed OA aging schemes, and the effect they have on predicted organic mass concentrations and O:C values. The base-case model configuration used here is an extension of the one-dimensional volatility basis set (1-D-VBS) and is described in detail in Murphy et al. (2011). That scheme reasonably reproduced summertime organic mass and O:C observations at Finokalia. The scheme approximates the effects of functionalizing organic compounds through oxidation by OH after formation of the first-generation semivolatile products (SOA and its attendant vapors) from traditional VOC oxidation. Each reaction is assumed to reduce saturation concentration by one order of magnitude and to add one or two oxygen atoms to the carbon skeleton with equal probability. For this case, an OH reaction rate constant equal to 1×10^{-11} cm^3 molec^{-1} s^{-1} will be applied to the condensable gases in equilibrium with traditional anthropogenic SOA. The parameterization for IVOC aging is based on the work of Grieshop et al. (2009), where the rate of 4×10^{-11} cm^3 molec^{-1} s^{-1} was found to reproduce smog-chamber formation of SOA from a diesel engine and wood cook-stove. In previous work (Murphy et al., 2009) it was assumed that the traditional SOA compounds would have smaller carbon number and thus to first order, smaller reaction rate with OH. This is not strictly true as the presence of oxygenated functional groups will affect the rate constant. Thus it is possible that the higher reaction rate for IVOCs is offsetting the erroneous fast initial formation of traditional VOCs. Consistent with Murphy et al. (2011), traditional biogenic condensable gases are aged at an equal rate to the traditional anthropogenic species, but reactions are assumed not to decrease their saturation concentrations, only increase their oxygen content, with functionalization and fragmentation in a rough balance. Other oxidants also play a role in SOA formation in the atmosphere. Indeed, this model includes condensable-gas production from oxidation of VOCs by ozone and nitrate radicals in addition to that by hydroxyl radicals. Once these species are formed, though, multigenerational aging by OH alone is assumed to be the dominant process degrading these compounds.

Another benefit of the 2-D-VBS framework is that this model explicitly describes the OM to OC ratio. Past studies (Shrivastava et al., 2008; Grieshop et al., 2009; Mur-

phy and Pandis, 2009; Farina et al., 2010; Hodzic et al., 2010) estimated the amount of organic mass added based on rough assumptions about the net addition of oxygen and possible hydrogen loss for each aging step. Because oxygen content is tracked by the O:C axis, total organic matter (OM) can be calculated online as described by Murphy et al. (2011). That study reported an average total organic mass addition of 16 % per OH oxidation reaction, but this value is somewhat variable.

The one-bin shift functionalization scheme just described has certain implications for the behavior of the OA population as a whole. First, because oxidation lowers saturation concentration one bin per reaction, if only homogenous gas-phase reactions are considered, SOA mass tends to accumulate in the saturation concentration bin corresponding to the total atmospheric loading (typically 0.1 to 10 µg m^{-3}). In other words, once the species condense they are no longer susceptible to oxidation, and will stay in this bin. The model will predict negligible SOA mass at effective saturation concentrations below 0.01 µg m^{-3}. Second, because only one direction of volatility transformation is considered, oxidation reactions will progressively move mass to lower volatility bins and enhance OA concentrations as an air parcel continues along its trajectory. This unyielding addition of mass is inconsistent with known chemistry (Atkinson and Arey, 2003; Kroll et al., 2009) and may lead to overestimation at medium to long aging time scales (Grieshop et al., 2009).

This study will address both of these concerns by first implementing a functionalization scheme that is based on group contribution methods to predict vapor pressures of likely products, followed by implementing a fragmentation scheme that takes into account C-C bond scission that likely occurs at moderate to high O:C.

3.2   Detailed functionalization scheme

This section describes the approach used to model functionalization of organic species in the 2-D-VBS. A more extensive explanation is given in Donahue et al. (2012b). An important underlying assumption here is that compounds under this model framework (with a certain C^* and O:C) are chemically similar enough to have a common average aging behavior during an aging reaction. It is for this reason that the model includes the initial step of oxidation of SOA precursors that is based on traditional SOA chamber yield parameterizations: explicitly modeled species have unique chemistry, but the products map into one of the 2-D-VBS classes described above. After the unique first-generation step, we hypothesize that aging is carried out primarily by reaction with OH and can be written as follows:

$$\text{ROG} + \text{OH} \rightarrow \sum_{i=1}^{N_O} \sum_{j=1}^{N_{C^*}} \alpha_{i,j} P_{i,j} \qquad (1)$$
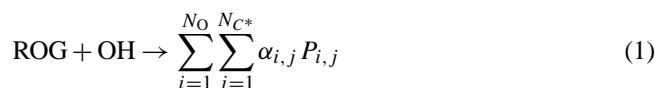
where ROG is a specific reactive organic gas and $\alpha_{i,j}$ is the stoichiometric yield of the product, $P_{i,j}$ with i oxygen atoms

Table 1. Stoichiometric yields* for the functionalization kernel applied to all species in the 2-D-VBS upon hydroxyl radical reaction.

$\Delta \log_{10} C^*$	-7	-6	-5	-4	-3	-2	-1
+3 O	0.02	0.04	0.08	0.04	0.02		
+2 O			0.05	0.15	0.20	0.10	
+1 O					0.06	0.15	0.09

* Product yields are on a carbon mass basis.

Table 2. Example stoichiometry for oxidation of organic vapor with O:C = 0.4 and $C^* = 10\,000\,\mu g\,m^{-3}$.

O:C	$\log_{10} C^*$							
	-3	-2	-1	0	1	2	3	4
0.9	0.004	0.010	0.018	0.010	0.004[a]			
0.8	0.022	0.043	0.087	0.043	0.022			
0.7			0.048	0.143	0.191	0.096		
0.6				0.038	0.078	0.093	0.040	
0.5					0.040	0.099	0.059	
0.4								ROG[b]

[a] Yields are on a total mass basis. The sum is equal to 1.2. [b] Carbon number inferred from group contribution methods is 7.2.

added relative to the organic gas parent and experiences a change in volatility by j volatility bins relative to the parent. N_{C^*} and N_O are the total number of volatility and O:C intervals, respectively. The number of oxygen atoms added per generation of oxidation, i, will vary depending on the particular chemical pathway followed. Here we assume that $N_O = 3$, with 50 % of the reaction adding two oxygen atoms ($\alpha_{2,j} = 0.5$ for all j), 20 % adding one ($\alpha_{1,j} = 0.2$ for all j), and 30 % adding three ($\alpha_{3,j} = 0.3$ for all j). Each number of added oxygens results in a different distribution of volatility reduction. Here, we use the trends outlined by Donahue et al. (2011) and informed by the SIMPOL group contribution methods developed by Pankow and Asher (2008). On average, each addition of an $-OH$ functionality should be accompanied by one $= O$ addition. This would lead to an average volatility reduction of -1.75 in $\log_{10} C^*$ per oxygen group added. Recognizing that this is an average, we center a distribution around this volatility change, and write an aging kernel that assigns products as a function of volatility and number of oxygen atoms added (Table 1). The kernel is applied to every organic surrogate species (every combination of saturation concentration and O:C). The transformation must be mapped from the kernel, which describes the number of added oxygens, to the y axis of the 2-D-VBS, which is O:C. Each point in the 2-D-VBS has a different average carbon number (Donahue et al., 2011) and thus will inform the translation from number of added oxygen atoms to change in O:C (Murphy et al., 2011). As an example, Table 2 shows the reaction stoichiometry that would result for a species with O:C = 0.4 and $C^* = 10\,000\,\mu g\,m^{-3}$. Coefficients in Table 1 are in carbon mass units and were transformed to total mass units online with the approach documented previously (Murphy et al., 2011). The coefficients in Table 2 are for total mass.

3.3 Detailed functionalization scheme with bSOA aging

For this detailed aging case, we relax the assumption that bSOA species age differently than their traditional anthropogenic SOA counterparts and treat all of the mass similarly after the first generation of oxidation. Previous work with PMCAMx-2008, a 3-D CTM, concluded that mass enhancement due to biogenic aging was probably already accounted for in the first-generation yield parameterization from chamber experiments (Murphy and Pandis, 2009, 2010). The ma-

jor evidence for this came from overprediction of OA mass at forested sites when enhancement from bSOA aging was considered. When bSOA was ignored and aSOA was allowed to age the model performed the best for both urban and rural, forested sites. Due to new evidence from chamber studies that biogenic SOA compounds do age (Ng et al., 2006; Tritscher et al., 2011), as well as field observations from radiocarbon analyses that find high contributions from modern (biogenic) carbon to the total OA mass (Szidat et al., 2006; Gilardoni et al., 2011; Yttri et al., 2011), we relax here our assumption and explore a scenario where biogenic SOA compounds age similarly to anthropogenic SOA compounds.

3.4 Fragmentation scheme

Breaking carbon bonds leads to products with lower carbon numbers than the parent, but not necessarily higher volatility since radical fragments will functionalize after they fragment. As described in the supplemental information of Donahue et al. (2012b), given that molecules of many structures exist in one surrogate species bin, it is likely that functional groups will exist in many locations throughout the carbon backbone. The locations of these functional groups will affect the probability of fragmenting at any given site, so we assume that this site of attack is on average randomly and thus uniformly distributed across the backbone as well. Since this uniform distribution acts on a molar basis, the mass distribution of the products will be weighted towards larger carbon number fragments. The O:C of the larger fragments will likely be similar to the O:C of the reactant hydrocarbon, and so these fragments will move directly right in the 2-D-VBS space, increasing in volatility but not in O:C. However, the smallest fragments will have a much larger O:C than the reactant. We represent this feature by assigning mass in all of the volatility bins to the right of the midpoint (from the reactant volatility bin to the highest modeled bin) O:C values that move diagonally towards the highest modeled O:C. Because some of these fragments will be radicals, we apply the functionalization kernel from Sect. 3.2 to a portion of those fragmentation products. The stable molecules remain at the

C^* and O:C values resulting from the first part of the fragmentation process.

The branching ratio between the functionalization and fragmentation pathways must also be parameterized. Highly reduced, large organic species typical of primary emissions and driving first-generation SOA formation are likely to only add functionalities rather than fragment upon oxidation. As they age, though, and functional groups are added along the backbone, fragmentation becomes more likely. Ultimately, oxidation must result in CO_2 if a mechanism were carried through to its thermodynamic endpoint. The fragmentation branching ratio is parameterized with the following relationship (Donahue et al., 2012a):

$$\beta_{\text{frag}} = (\text{O:C})^{(1/6)} \tag{2}$$

The branching ratio, β_{frag}, equals 0 if the compound has no oxygen and only functionalizes upon oxidation. β_{frag} will equal 1 if the reactant compound is so oxygenated that almost all of the products are fragmented when reacted with OH. This dependence on O:C ensures that compounds will most likely fragment after reaching O:C = 0.4.

3.5 Condensed-phase aging

Two additional sensitivity cases to the detailed model configuration employing functionalization and fragmentation will be explored: (1) OH uptake and reaction in the particle phase, and (2) aqueous-phase SOA formation.

In addition to degrading gas-phase organic compounds, hydroxyl radicals can also collide with particles and react with OA molecules in the particle phase (or on the particle surface). This study uses the same theoretical assumptions that appeared in Murphy et al. (2011). The model does not explicitly account for the size dependence of OH uptake; instead it simulates this reaction similarly to the gas-phase mechanism but with a reduced rate constant ($k_{\text{OH}} = 6 \times 10^{-12}$ cm^3 molec^{-1} s^{-1}) to account for rate limitations due to diffusion (Weitkamp et al., 2008). This value is suggested as an upper bound by Jimenez et al. (2009) and Donahue et al. (2012b), and is a factor of 3 larger than that used in previous work (Murphy et al., 2011), in which this heterogeneous process was found not to affect either predicted OA concentrations or O:C significantly at Finokalia during the summer period. The rate constant is increased by a factor of 3 to try to reveal a signal in the model and determine whether or not the process might be important. The products from each heterogeneous OH reaction are distributed with the same aging kernels applied to the gas-phase aging reactions. This is a source of uncertainty but little information exists regarding product distributions of heterogeneous-phase OH chemistry. Particle-phase reactions between organic compounds may also be important for producing low-volatility species like oligomers or organosulfates that enhance OA mass. However, these reactions are not considered in this work due to the uncertainty in their reac-

tion rates and products (Hallquist et al., 2009). Also, these particle-phase reactions will not enhance O:C in the particle phase, unless significant fragmentation and volatilization of the more hydrocarbon-like fragment occurs. This trend is not supported by the current evidence (Hallquist et al., 2009).

Aqueous-phase chemistry is considered here for the dissolution of glyoxal and methylglyoxal into the particulate aqueous phase followed by reaction with the hydroxyl radical to form oxalic acid and oxalic-acid like products (Carlton et al., 2008; Myriokefalitakis et al., 2011). The solubilities of glyoxal and methylglyoxal are parameterized through their effective Henry's law constants (3×10^5 and 3.7×10^3 M atm^{-1}, respectively). This aqueous-phase mass reacts with aqueous OH ($H^{\text{eff}} = 25$ M atm^{-1}; Seinfeld and Pandis, 2006) to form oxalic acid with a reaction rate constant of 3.1×10^9 mol^{-1} s^{-1} (Myriokefalitakis et al., 2011). This OA mass is subject to wet and dry deposition in the host transport model after formation. We assume O:C = 1.7 for SOA from glyoxal and 1.5 for that from methylglyoxal, consistent with chamber experiments (Ervens et al., 2011).

4 Results

4.1 Base-Case functionalization scheme

The base-case scheme presents a relatively simple approach to aging chemistry, yet it reproduces diurnally averaged OA concentrations and O:C at the three EUCAARI sites reasonably well in both seasons (Fig. 1a, b). The model predicts OA concentrations better for summer conditions than winter at all three sites, with fractional error not exceeding 35 % for summer (Table 3). For winter, the base-case model performs similarly for Finokalia and Cabauw, but overpredicts in Mace Head (fractional error = 88 %). Fractional biases indicate overestimation of OA mass concentrations during both seasons at Finokalia and Cabauw, with stronger overestimation during the winter. The Mace Head OA mass concentrations are consistently overpredicted in the winter time (fractional bias = 84 %). The root-mean-square-error for this particular dataset is also the worst, indicating possible problems with the winter emissions inventory near Ireland, or a problem with the application of the IVOC emission parameterization to sources in Western Europe. Otherwise, the base-case model appears to be behaving consistently throughout a range of low to moderate organic mass loadings.

O:C (Table 4) predictions are in moderate agreement with measurements(fractional error $\leq$ 28 %, fractional bias $\leq \pm 28$ %). The absolute magnitude of O:C predicted, which varies from 0.34 to 0.66, is also in agreement with AMS observations reported by Ng et al. (2010). Oxygenation is clearly underpredicted at Finokalia during the summer period. This result was seen in previous work (Murphy et al., 2011), but it was also noted that biases in the conversion from m/z 44 (measured by the AMS) to O:C could introduce up to
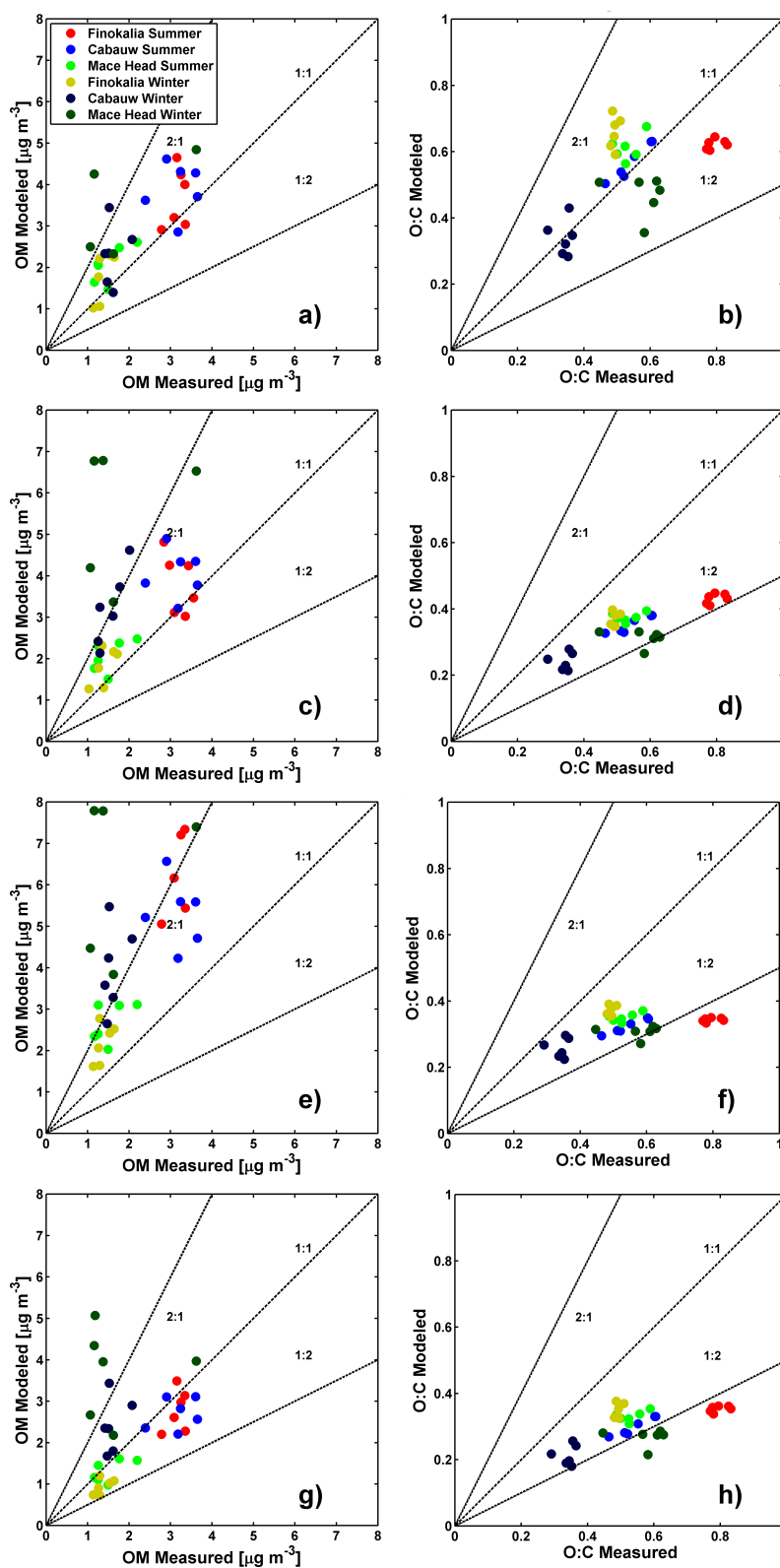
Fig. 1. Model-measurement agreement for OA mass concentrations (left column) and O:C (right column) at all three observation sites for both summer and winter seasons. Each row corresponds to a specific model implementation: base case (top row), detailed functionalization case (second row), detailed functionalization with bSOA aging (third row), and functionalization plus fragmentation case (bottom row).

Table 3. Organic mass concentration (μg m^{-3}) performance metrics for all simulations.

Season	Site	Model Run	Meas. Avg	Sim. Avg	Fract. Error	Fract. Bias	RMSE
Summer	Finokalia	Base case	3.07	3.67	0.18	0.14	0.80
		Func.		3.82	0.20	0.16	1.03
		Func. with bSOA age		6.38	0.69	0.69	3.43
		Func./Frag.		2.66	0.16	−0.15	0.57
		Het. OH Uptake		2.73			
		Aq-Phase Production		2.67			
	Cabauw	Base case	3.18	3.90	0.24	0.20	1.02
		Func.		4.07	0.25	0.25	1.14
		Func. with bSOA age		5.32	0.50	0.50	2.34
		Func./Frag.		2.70	0.19	−0.16	0.70
		Het. OH Uptake		2.43			
		Aq-Phase Production		2.71			
	Mace Head	Base case	1.43	2.06	0.35	0.35	0.71
		Func.		2.07	0.31	0.31	0.64
		Func. with bSOA age		2.68	0.60	0.60	1.31
		Func./Frag.		1.32	0.16	−0.08	0.28
		Het. OH Uptake		1.17			
		Aq-Phase Production		1.34			
Winter	Finokalia	Base case	1.33	1.77	0.31	0.24	0.60
		Func.		1.82	0.27	0.25	0.53
		Func. with bSOA age		2.17	0.47	0.47	0.91
		Func./Frag.		0.95	0.34	−0.34	0.42
		Het. OH Uptake		0.72			
		Aq-Phase Production		0.96			
	Cabauw	Base case	1.56	2.31	0.39	0.35	0.97
		Func.		3.20	0.68	0.68	1.76
		Func. with bSOA age		3.99	0.85	0.85	2.57
		Func./Frag.		2.42	0.41	0.41	1.01
		Het. OH Uptake		2.26			
		Aq-Phase Production		2.44			
	Mace Head	Base case	1.92	4.34	0.88	0.84	2.91
		Func.		5.96	1.12	1.12	4.66
		Func. with bSOA age		6.83	1.18	1.17	5.42
		Func./Frag.		3.70	0.80	0.73	2.53
		Het. OH Uptake		3.38			
		Aq-Phase Production		3.75			

20 % uncertainty in the observations. Still, the model reproduces the trend of higher O:C ratios with longer transport times from sources that is seen in the ambient data.

The volatility distributions shown in Fig. 2a and b correspond to the average state of OA and organic vapor mass of parcels arriving at the Cabauw ground site at 9 a.m. and 6 p.m. local time, respectively. These distributions illustrate an important feature of the simple scheme used for this base case. These figures are snapshots of different parcels at one location (Cabauw) rather than of the same air parcel as it continues to be oxidized, but the basic trend is captured. Organic vapor mass is freshly emitted in the morning hours throughout a range of saturation concentrations, and by the afternoon

it is pushed largely into the 0.1 and 1 μg m^{-3} bins. Moreover, a great deal of vapor mass is not aged to lower volatility. These are the biogenic secondary organic vapors. If these were aged under this scheme, the model would likely overpredict OA concentrations at all sites as was seen in Murphy et al. (2011). Figure 3 shows the O:C distribution of parcels arriving at Finokalia at 1 p.m. local time averaged over all simulation days for each of the these three scenarios. The base-case scenario predicts O:C values that peak in the mid-afternoon and generally increase as the parcel proceeds along its trajectory, which is consistent with the picture of the atmosphere as an oxidizing environment for organic molecules. Given AMS measurements that separate OOA into SV-OOA

Table 4. O:C performance metrics for all simulations.

Season	Site	Model Run	Meas. Avg	Sim. Avg	Fract. Error	Fract. Bias	RMSE
Summer	Finokalia	Base case	0.80	0.62	0.25	−0.25	0.18
		Func. with bSOA age		0.43	0.59	−0.59	0.37
		Func.		0.34	0.79	−0.79	0.45
		Func./Frag.		0.35	0.77	−0.77	0.44
		Het. OH Uptake		0.46			
		Aq-Phase Production		0.35			
	Cabauw	Base case	0.54	0.57	0.05	0.05	0.03
		Func. with bSOA age		0.35	0.42	−0.42	0.19
		Func.		0.32	0.50	−0.50	0.22
		Func./Frag.		0.30	0.57	−0.57	0.24
		Het. OH Uptake		0.37			
		Aq-Phase Production		0.31			
	Mace Head	Base case	0.53	0.61	0.15	0.15	0.09
		Func. with bSOA age		0.37	0.34	−0.34	0.16
		Func.		0.35	0.40	−0.40	0.18
		Func./Frag.		0.33	0.46	−0.46	0.20
		Het. OH Uptake		0.41			
		Aq-Phase Production		0.36			
Winter	Finokalia	Base case	0.49	0.66	0.28	0.28	0.17
		Func. with bSOA age		0.37	0.29	−0.29	0.13
		Func.		0.37	0.28	−0.28	0.12
		Func./Frag.		0.35	0.35	−0.35	0.15
		Het. OH Uptake		0.40			
		Aq-Phase Production		0.37			
	Cabauw	Base case	0.34	0.34	0.14	−0.01	0.05
		Func. with bSOA age		0.24	0.34	−0.34	0.10
		Func.		0.26	0.28	−0.28	0.09
		Func./Frag.		0.21	0.46	−0.46	0.13
		Het. OH Uptake		0.23			
		Aq-Phase Production		0.24			
	Mace Head	Base case	0.58	0.47	0.24	−0.21	0.14
		Func. with bSOA age		0.31	0.59	−0.59	0.27
		Func.		0.31	0.60	−0.60	0.28
		Func./Frag.		0.27	0.72	−0.72	0.32
		Het. OH Uptake		0.29			
		Aq-Phase Production		0.29			

and low volatility OOA (LV-OOA), one might expect most OA mass at Finokalia to fall within a tight range of high O:C representative of a high degree of aging (Hildebrandt et al., 2010a). Instead, the model-predicted O:C distribution of the parcel as it arrives at the observation site (far right of Fig. 3a) does not indicate that most OA at Finokalia was aged to high O:C but rather that a heavy tail of mass dispersed in O:C space enhances the O:C weighted average. This may indicate a weakness in the base-case model's ability to represent OA aging chemistry accurately or it may reveal a different perspective of ambient OA worth investigating in field measurements. The figure also shows an accumulation of mass at very high O:C. As mentioned before, this model assumes

that bSOA volatility is not affected by aging. Thus most of the aged bSOA vapors have plenty of opportunity to continue to age in the gas-phase and contribute to these highly oxygenated species.

4.2 Detailed functionalization scheme

The functionalization kernel constitutes an attempt to more accurately represent the effect that addition of alcohol, carbonyl, and acid functionality to the carbon backbone will have on the volatility of typical atmospheric organic compounds. The products of this kind of oxidation pathway will likely reduce in saturation concentration by an average of 1.7 decades per added oxygen (3.4 decades per generation),

significantly lower than assumed in the base-case model (1 decade per generation). As a consequence, organic mass beginning at high volatility with little contribution to the condensed phase (i.e. $C^* > 10\,\mu g\,m^{-3}$) moves to lower volatility with fewer OH reactions necessary, thereby enhancing bulk OA concentrations. This is evident at Cabauw and Mace Head in the winter (Fig. 1 and Table 3). It is interesting that for many cases in this study, it is difficult to see a difference in predicted OA mass concentration between this case and that of the base case. This highlights the importance of using metrics other than OA mass (O:C, volatility) to constrain OA aging mechanisms. Otherwise it will be very difficult to evaluate one model's performance over another. There are many ways to get the same right answer for different reasons.

The effect of this scheme on predicted O:C is striking. Because, in this model configuration, fewer generations of oxidation are necessary to yield low volatility OA, the average O:C of OA formed decreases substantially (almost a factor of 2 at all sites and seasons). The predicted average O:C falls between 0.24 and 0.43, which is characteristic of semi-volatile oxygenated organic aerosol (SV-OOA) observed in the atmosphere (Ng et al., 2010), but significantly lower than that for bulk OA.

4.3 Detailed functionalization scheme with bSOA aging

Predicted organic aerosol concentrations using the functionalization scheme with net bSOA aging increase and are biased high with a fractional bias reaching 69 % during the summer in Finokalia and 117 % during the Mace Head winter. Much of the OA concentration enhancement seen in the resulting prediction comes from aging of this bSOA mass. The most extreme example is at Finokalia during the summer, where the average concentration of bSOA mass increases from $0.94\,\mu g\,m^{-3}$ in the base case to $3.73\,\mu g\,m^{-3}$ in the detailed functionalization case ($\sim 300\,\%$ enhancement). The predicted enhancement in aSOA mass is comparatively modest, $0.62\,\mu g\,m^{-3}$ to $0.82\,\mu g\,m^{-3}$ ($\sim 32\,\%$ enhancement).

This parameterization predicts an O:C trend that stays relatively constant throughout the evolution of the air parcel (Fig. 3b). The magnitude at which O:C is constant depends on both the functionalization kernel (saturation concentrations reduction per OH reaction) and the assumed extent of oxidation of the 1st-generation SOA products. Whereas some mass continues to age up to O:C = 0.6–0.7, more mass is added at low O:C values from freshly emitted POA and recently oxidized SOA, and the bulk average O:C stays relatively constant, despite daily changes in meteorological conditions and variable emissions sources along the parcel path.

4.4 Fragmentation scheme

Scission of carbon-carbon bonds due to oxidation may be an important process to atmospheric organic compound evolution but its overall effects are complex and uncertain. Our

representation of the fragmentation phenomenon results in significant changes to predicted organic mass concentrations but not to O:C (Fig. 1) when compared to the detailed functionalization case. Bond cleavage results in product species with fewer carbons than the reactant molecule. Even though subsequent functionalization of these fragments may very well lead to products with lower volatility than the reactant, the average effect of fragmentation is to increase volatility, as expected. This drives a decrease of OA concentrations compared to the detailed functionalization case. The fragmentation scenario predicts OA concentrations more similar to the base-case model configuration, although concentrations are substantially lower (generally 0.6–$1.0\,\mu g\,m^{-3}$ less) for all cases except Cabauw winter, where concentrations slightly increased. The detailed functionalization/fragmentation scenario includes more dynamic pathways for the evolution of aged products (they may increase or decrease in volatility and O:C by varying magnitudes depending on their location in the 2-D-VBS space), and from an OA mass concentration perspective, these effects lead to closer agreement with ambient measurements.

Although OA mass concentration predictions seem to be within reason, the model fails to predict the degree of oxygenation observed during the EUCAARI study. Fractional biases (FB) are between $-77\,\%$ and $-35\,\%$, following closely the detailed functionalization case. The two worst performing periods were summer in Finokalia (FB = $-77\,\%$) and winter in Mace Head (FB = $-72\,\%$), indicating that this scenario is deficient in representing aging over long time scales while pollutants are being transported to remote sites. The model performs marginally better in suburban Cabauw (FB = $-57\,\%$ and $-46\,\%$ in summer and winter, respectively), but there is still a clear discrepancy in the representation of oxidation chemistry as O:C is underpredicted by a little more than half even in this location that is close to sources. This case also predicts a rather constant O:C (Fig. 3d) evolution along parcel trajectories, comparable to the previous case, which does not consider fragmentation. Mass concentrations are suppressed by added evaporation when fragmentation is introduced, and this evaporation becomes much more likely after compounds reach O:C = 0.4, explaining why the bulk-average O:C does not grow beyond this level. There is some mass growth at high O:C (~ 1.2), but this mass is a feature of the modeling framework functionalizing highly volatile ($C^* \geq 10^6\,\mu g\,m^{-3}$) compounds.

4.5 Condensed-phase aging

4.5.1 Heterogeneous reaction via OH Uptake

The effects of particle-phase OA oxidation by OH uptake on total mass loadings are variable but relatively modest. One case (Finokalia summer) shows OA particulate mass enhancement, due to particle-phase reactions driving mass to even lower volatility, while other cases result in decreases in
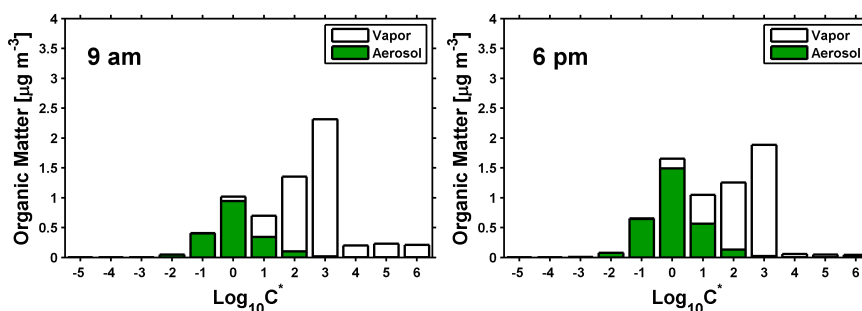
Fig. 2. Modeled volatility distributions as a function of effective saturation concentration for parcels arriving at Cabauw, Netherlands during the summer episode. The data is an average over all simulation days during the campaign.

mass loadings when this chemistry is added (Table 3). These decreases are due to volatilization of aged organic species from the particle phase. This sensitivity study illustrates the considerable complexity that heterogeneous oxidation processes introduce in conceptual models of atmospheric OA aging. The overall effect these processes have on organic particulate loadings is a function of several variables. The age of the parcel, the specific anthropogenic or biogenic sources involved, the OA mass loading, the O:C distribution, and local meteorological conditions all seem to play a role. Noting these complications, though, the net effect of heterogeneous chemistry via particle-phase OH reactions was not greater than $\pm 0.4 \, \mu g \, m^{-3}$ in any simulation in this study, even with the upper-bound estimation of the particle-phase OH reaction rate constant. These reactions have a more significant, and consistent effect on the degree of OA oxygenation though. Because oxidation can occur in both the particulate- and gas-phases and O:C increases with every reaction, it is enhanced for every case investigated here (Table 4). Enhancements in O:C appear to be strongly correlated with exposure to high photochemical activity, as expected. The strongest increases are seen during summer periods at all sites and at low latitudes during the winter (O:C in Finokalia increases from 0.35 to 0.46), where there is more sunlight. The absolute magnitude of the increase (typically ~ 0.1) even at suburban Cabauw in the summertime motivates further investigation of these processes, keeping in mind that the rate of reaction assumed is high compared to what laboratory studies suggest.

Figure 3d shows that for this scenario, as in the base case, O:C continues to increase as the parcel is transported toward its destination. This is mostly due to a build-up of mass high in O:C (~ 1.1). This mass is oxidized in the particle phase but does not volatilize. A major source of uncertainty in this effort is the assumption that heterogeneous- and gas-phase reactions can be modeled with the same aging kernels. It is quite possible that chemistry in the condensed-phase would lead to formation of different products than that in the gas-phase. Thus, the model configuration used here is only a first guess.

4.5.2 Aqueous-phase SOA formation

This scenario includes formation of SOA by glyoxal and methylglyoxal absorbed into cloud water and reacted with hydroxyl radicals absorbed into the same phase. Formation of these precursor species in the gas-phase by oxidation of hydrocarbons is parameterized by the SAPRC-99 chemical mechanism. Overall, glyoxal formed about two orders of magnitude more OA mass than methylglyoxal in all cases. This was expected given their significant difference in effective Henry's law constants. Negligible enhancements to both OA mass loadings ($\leq 3\%$) and O:C ($\leq 10\%$) at the surface were seen for the diurnally-averaged, representative days at all sites when this chemical pathway was added to the detailed functionalization/fragmentation scenario. However, OA mass enhancement on some specific days was significantly higher than the average increase. For example, on 17 March at Mace Head, $0.1 \, \mu g \, m^{-3}$ was formed by glyoxal processing, which is about 10 times the average formation seen for the representative day evaluated in winter at that site.

The OA production from this scenario is somewhat lower than that seen by Carlton et al. (2008), where monthly average carbon mass was increased by $\sim 0.2 \, \mu g C \, m^{-3}$ at Speciation Trends Network (STN) and IMPROVE measurement sites in the Eastern United States. It is also lower in absolute magnitude than estimates from observations of glyoxal during the recent CalNEX campaign, where 0–$0.2 \, \mu g \, m^{-3}$ organic matter was attributed to glyoxal processing (Washenfelder et al., 2011). However, the relative contribution estimated from that study was 0–4% of total SOA mass formed, which is similar to the results here. Another important consideration in comparing results among aqueous-phase processing studies is the episodic nature of this phenomenon that has been observed. Carlton et al. (2008) point out that meteorology, including cloud field variability can play a significant role in model predictions. The current results indicate that aqueous-phase processing may not be as important from a regional, highly averaged perspective. Thus individual model studies should be compared with each other and with measurements for the same time and location.
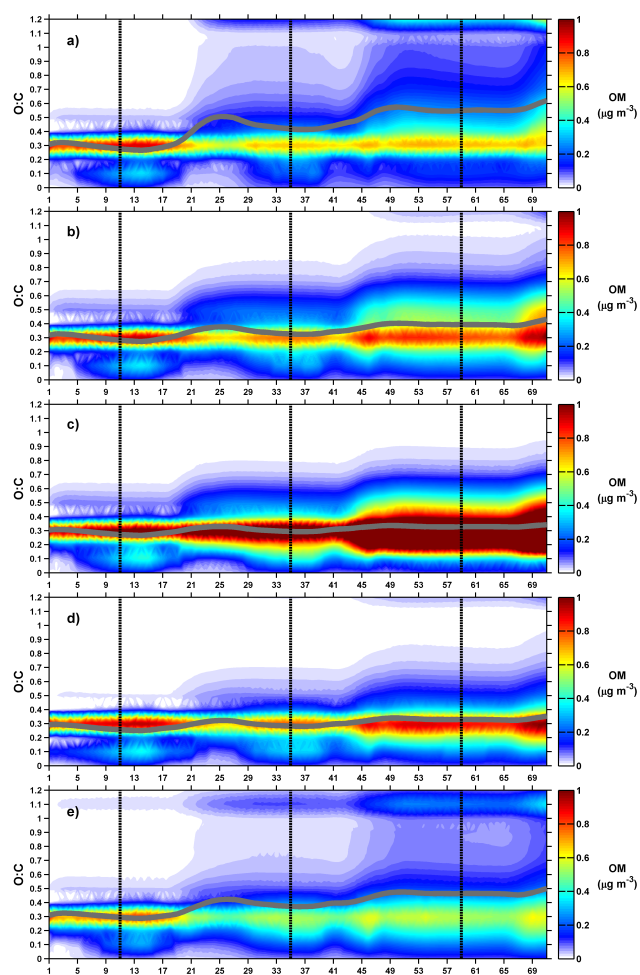
Fig. 3. Average modeled O:C distribution as parcels approach Finokalia in the summer time. The x-axis corresponds to time along the trajectory approaching Finokalia (parcels are initialized at $t = 1$ and arrive at the site at $t = 71$ h). Four scenarios are shown: **(a)** base case, **(b)** detailed functionalization, **(c)** detailed functionalization with bSOA aging, **(d)** detailed functionalization/fragmentation and **(e)** detailed functionalization/ fragmentation with heterogeneous chemistry via OH uptake. Parcels arrive at 1 p.m. local time. The gray line indicates the concentration-weighted O:C ratio for bulk organic aerosol predicted by the 2-D-VBS model. The dashed black vertical lines indicate midnight during the trajectory.

5 Discussion

When viewed together, the base-case, detailed functionalization and detailed functionalization/fragmentation scenarios explored in this study reveal interesting features regarding the current concept of OA aging. The base-case model has weaknesses due to its chemical simplicity. It can be criticized for accumulating OA mass in the semivolatile regime that is acceptable over the course of a laboratory experiment but may lead to mass overprediction at atmospherically-relevant timescales. However, the model has performed well in CTM evaluations after certain assumptions (i.e. no net effect of ag-

ing on volatility of bSOA) were introduced (Lane et al., 2008; Murphy and Pandis, 2009; Tsimpidi et al., 2010; Fountoukis et al., 2011). The detailed functionalization scenario employs the fundamentals of group contribution theory to approximate the effect on volatility of adding relevant functional groups to the carbon backbone (Donahue et al., 2011). This approach results in OA overprediction and O:C underprediction in every case examined in this dataset and is therefore not likely representing the whole aging story on its own.

Fragmentation may be an important process causing overall loss of OA mass for an ensemble of compounds. However, the specific effect of fragmentation on individual species may not be to increase volatility, especially for large, reduced compounds. Adding this chemical pathway to the detailed functionalization scenario decreased OA mass concentrations to the approximate magnitude predicted by the base-case and brought the model into closer agreement with the OA mass concentration measurements. Because source contributions are variable among the sites and seasons used in this study (Fig. 4), it would be fair to hypothesize that this detailed functionalization/fragmentation scheme would predict bulk OA concentrations similar to the full 3-D version of PMCAMx-2008, which employs an organic aging module consistent with that of the base case.

There are other important concerns to be addressed though. First, the base-case and detailed functionalization/fragmentation models predict very different O:C trends along a parcel trajectory. Fragmentation acts as a sink for moderately oxidized compounds in removing them from the particle phase through volatilization according to the branching ratio calculated (Eq. 2). Reduced compounds are not as susceptible to this process so they provide an additional source for aerosol mass at lower O:C. With a source and sink in place, a trend similar in behavior to a pseudo-steady-state develops and O:C stays relatively constant along a parcel trajectory. The base case does not include a fragmentation sink, and thus accumulation of O:C and OA mass is evident as air parcels age. Because the detailed fragmentation/functionalization case incorrectly predicts low O:C values, it can be inferred that important OA production mechanisms are either missing from the model or incorrectly related to the 2-D-VBS space. Therefore, readers are cautioned not to blindly apply these organic aerosol aging parameterizations without evaluation of their applicability to the system of interest.

The second concern addresses apportionment of OA to its sources, an important issue to understand when recommending, adopting and enforcing air quality standards. Figure 4 reemphasizes the relative agreement between the base case and detailed functionalization/fragmentation case, especially when compared to the enhanced OA mass concentrations for the detailed functionalization with biogenic SOA aging. However, this gross agreement is not always achieved for the same reasons. For example, although the Mace Head winter case shows similar fractional contribution among the
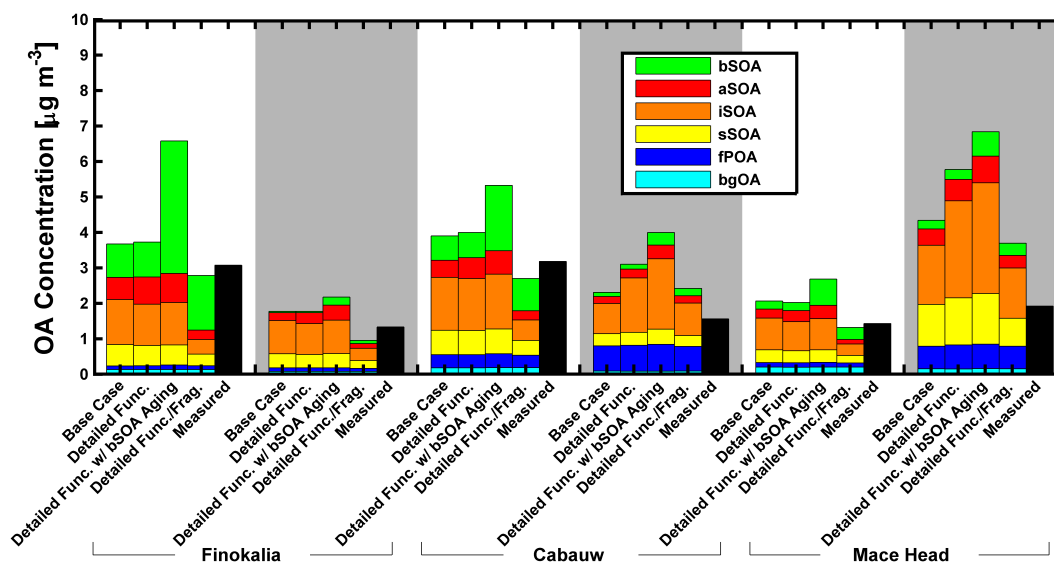
Fig. 4. Simulation average OA mass concentrations resolved by source class. Data on white backgrounds are for summer scenarios while shaded backgrounds indicate winter scenarios.

source categories isolated by the model for the base case and detailed functionalization/fragmentation case, the summertime Finokalia illustrates high discrepancy, where bSOA contributes 65 % of the OA mass to the system when it is aged, while it makes up only 20 % for the base case model configuration. In fact, most sites show this rough doubling of the fractional contribution of biogenic SOA to the total when aging is explicitly accounted for with the 2-D-VBS approach. Biogenic SOA dominates over traditional anthropogenic sources of SOA (e.g. toluene, xylene, alkenes, alkanes, etc.) for all summer-time scenarios when fragmentation is treated similarly for both surrogates. In most cases though, summer and winter, more than half of the total OA mass is predicted to originate from anthropogenic sources, which includes traditional SOA, intermediate volatility SOA, semivolatile SOA and POA. There are also uncertainties about the role of NO_x (anthropogenic) in enhancing bSOA growth. Above all it is important for policy applications to have an understanding of how much ambient OA loadings can be reduced by reducing anthropogenic emissions.

These source-resolved results can be compared to existing literature reporting observations at sites in Europe (Szidat et al., 2006; Gelencser et al., 2007; Gilardoni et al., 2011; Yttri et al., 2011). These studies focus on distinguishing fossil from non-fossil carbon measured at field sites using radiocarbon analysis and then using levoglucosan/OC and fossil EC/OC ratios to calculate the contributions of biomass burning and fossil fuel POA, respectively, to the total carbon. The remainder, after subtracting biomass burning OC from non-fossil organic carbon and fossil fuel POA from fossil organic carbon, is the contribution of biogenic SOA and anthropogenic SOA, respectively. Gelencser et al. (2007) report that about 63–76 % of total carbon is SOA from non-fossil

sources. Szidat et al. (2006) found this fraction to be lower in the winter for Zurich (27 %) and about as high in the summer (60 %). Fossil fuel source contributions for that study were stable throughout the year (around 30 %). Yttri et al. (2011) found consistent results in Scandinavia with 50–57 % of total carbon coming from non-fossil SOA sources, but only about 10 % from fossil fuel sources. Simpson et al. (2007) performed a forward-model exercise with the European Monitoring and Evaluation Programme (EMEP) MSC-W model, but did not find the same strong contribution to total organic carbon from biogenic SOA sources, predicting instead the greatest contributions at measurement sites to be from fossil primary organic carbon. The present work falls somewhat between these two perceptions, as shown in Fig. 4. The base case and detailed functionalization models perform similarly for most sites and seasons, especially during the summer when IVOC emissions are lower. For these scenarios, bSOA contributes 20 % or less to the total OA mass concentration. Additional non-fossil components (e.g. from agricultural activities) are included in the fPOA, sSOA, iSOA components as well as in the OA transported into the domain from elsewhere (bgOA). When bSOA aging and fragmentation is included bSOA accounts for around 65 % of the total OA mass concentration as mentioned above. This second estimate seems to be in better agreement with the radiocarbon studies, and may point to a step in the right direction in implementing aging and fragmentation for bSOA compounds. However, it is also true that those studies assume levoglucosan to be a non-volatile, unreactive compound which may not be true under atmospheric conditions. If biomass burning contributions are underpredicted in those studies, then contributions from bSOA are overpredicted. Regardless, the suite of aging modules chosen for this work have shown that

the 2-D-VBS framework is capable of reproducing reality as these uncertainties are constrained in the future.

6 Conclusions

This work presented the continued development and evaluation of the 2-D-VBS framework with ambient observations from the EUCAARI campaign. The model was evaluated for its ability to predict OA mass concentrations and O:C at two remote sites and one suburban site for two seasons. The base-case aging configuration, which employed a simplified functionalization scheme designed only to reduce the volatility of organic species by one decade in saturation concentration upon gas-phase OH oxidation, predicted OA concentrations moderately well (fractional error $\leq 40\%$, fractional bias $\leq \pm 35\%$) for all sites except Mace Head in the winter time. O:C was predicted well at all sites, especially given the variability in O:C seen at each site throughout the year.

Two other schemes were developed to explore the roles of more detailed parameterizations of functionalization and fragmentation processes. The detailed functionalization case overpredicted OA concentrations at all sites and underpredicted O:C ratios considerably. This is a direct result of the assumed shift of -1.75 in $\log_{10}C^*$ for every functional group added. With functionalization and fragmentation invoked for all SOA species (including biogenic SOA), the model predicted less OA mass concentrations than the base case and the detailed functionalization case. Statistically, this scheme showed the best performance for OA mass concentration predictions during the summer. However, it performed worse than the base-case scheme at predicting O:C. It is possible that some other process not present in this model contributes to the enhanced degree of oxygenation seen at photochemically intense, remote sites like Finokalia.

Heterogeneous reaction with OH in the particle phase, and aqueous-phase production of oxalic acid from glyoxal and methylglyoxal were both explored to try to close the gap in O:C predictions of the functionalization/fragmentation scheme. Heterogeneous reactions (an upper bound parameterization) enhanced O:C by continuing to oxidize particle-bound species, but also served to decrease OA concentrations during several periods due to fragmentation and evaporation out of the particle phase. Aqueous-phase production of oxalic acid did not produce enough highly oxygenated OA to close the modeled/measurement gap in O:C either.

Further understanding of the full OA aging mechanism is important for fundamental understanding of OA atmospheric chemistry but also policy decision making. The 2-D-VBS is a useful conceptual framework for organizing atmospheric organic chemistry into a relatively concise picture. It is also readily evaluated with physical observations of ambient and laboratory particles through the use of the AMS and thermodenuder. However, large uncertainties still loom for this approach, including the parameterization for the functional-

ization/fragmentation branching ratio and the nature of the chemistry that may be occurring in the particle phase. Future laboratory work is needed to explore these phenomena and identify other processes that could account for the high degree of oxygenation seen in summertime Finokalia where transport times are long and photochemistry is substantial. In general the 2-D-VBS space is a great utility for exploring these uncertainties as lessons learned from laboratory studies are connected to field observations.

References

Aiken, A. C., Decarlo, P. F., Kroll, J. H., Worsnop, D. R., Huffman, J. A., Docherty, K. S., Ulbrich, I. M., Mohr, C., Kimmel, J. R., Sueper, D., Sun, Y., Zhang, Q., Trimborn, A., Northway, M., Ziemann, P. J., Canagaratna, M. R., Onasch, T. B., Alfarra, M. R., Prevot, A. S. H., Dommen, J., Duplissy, J., Metzger, A., Baltensperger, U., and Jimenez, J. L.: O/C and OM/OC ratios of primary, secondary, and ambient organic aerosols with high-resolution time-of-flight aerosol mass spectrometry, Environ. Sci. Technol., 42, 4478–4485, doi:10.1021/Es703009q, 2008.

Atkinson, R. and Arey, J.: Atmospheric degradation of volatile organic compounds, Chem. Rev., 103, 4605–4638, doi:10.1021/Cr0206420, 2003.

Aumont, B., Szopa, S., and Madronich, S.: Modelling the evolution of organic carbon during its gas-phase tropospheric oxidation: development of an explicit model based on a self generating approach, Atmos. Chem. Phys., 5, 2497–2517, doi:10.5194/acp-5-2497-2005, 2005.

Bergström, R., Denier van der Gon, H. A. C., Prévôt, A. S. H., Yttri, K. E., and Simpson, D.: Modelling of organic aerosols over Europe (2002–2007) using a volatility basis set (VBS) framework: application of different assumptions regarding the formation of secondary organic aerosol, Atmos. Chem. Phys., 12, 8499–8527, doi:10.5194/acp-12-8499-2012, 2012.

Carlton, A. G., Turpin, B. J., Altieri, K. E., Seitzinger, S. P., Mathur, R., Roselle, S. J., and Weber, R. J.: CMAQ model performance enhanced when in-cloud secondary organic aerosol is included: comparisons of organic carbon predictions with measurements, Environ. Sci. Technol., 42, 8798–8802, doi:10.1021/Es801192n, 2008.

Chacon-Madrid, H. J., Presto, A. A., and Donahue, N. M.: Functionalization vs. fragmentation: n-aldehyde oxidation mechanisms

and secondary organic aerosol formation, Phys. Chem. Chem. Phys., 12, 13975–13982, doi:10.1039/C0cp00200c, 2010.

Chen, Q., Liu, Y. J., Donahue, N. M., Shilling, J. E., and Martin, S. T.: Particle-phase chemistry of secondary organic material: modeled compared to measured O:C and H:C elemental ratios provide constraints, Environ. Sci. Technol., 45, 4763–4770, doi:10.1021/Es104398s, 2011.

Chhabra, P. S., Flagan, R. C., and Seinfeld, J. H.: Elemental analysis of chamber organic aerosol using an aerodyne high-resolution aerosol mass spectrometer, Atmos. Chem. Phys., 10, 4111–4131, doi:10.5194/acp-10-4111-2010, 2010.

Dall'Osto, M., Ceburnis, D., Martucci, G., Bialek, J., Dupuy, R., Jennings, S. G., Berresheim, H., Wenger, J., Healy, R., Facchini, M. C., Rinaldi, M., Giulianelli, L., Finessi, E., Worsnop, D., Ehn, M., Mikkila, J., Kulmala, M., and O'Dowd, C. D.: Aerosol properties associated with air masses arriving into the North East Atlantic during the 2008 Mace Head EUCAARI intensive observing period: an overview, Atmos. Chem. Phys., 10, 8413–8435, doi:10.5194/acp-10-8413-2010, 2010.

Denier van der Gon, H. A. C., Visschedijk, A., and Zandveld, P.: EUCAARI Report No. 036833-2: Pan-European carbonaceous aerosol inventory, TNO Built Environment and Geosciences, Utrecht, The Netherlands, 2009.

Donahue, N. M., Robinson, A. L., Stanier, C. O., and Pandis, S. N.: Coupled partitioning, dilution, and chemical aging of semivolatile organics, Environ. Sci. Technol., 40, 2635–2643, doi:10.1021/Es052297c, 2006.

Donahue, N. M., Epstein, S. A., Pandis, S. N., and Robinson, A. L.: A two-dimensional volatility basis set: 1. Organic-aerosol mixing thermodynamics, Atmos. Chem. Phys., 11, 3303–3318, doi:10.5194/acp-11-3303-2011, 2011.

Donahue, N. M., Kroll, J. H., Pandis, S. N., and Robinson, A. L.: A two-dimensional volatility basis set – Part 2: Diagnostics of organic-aerosol evolution, Atmos. Chem. Phys., 12, 615–634, doi:10.5194/acp-12-615-2012, 2012a.

Donahue, N. M., Henry, K. M., Mentel, T. F., Kiendler-Scharr, A., Spindler, C., Bohn, B., Brauers, T., Dorn, H. P., Fuchs, H., Tillmann, R., Wahner, A., Saathoff, H., Naumann, K.-H., Möhler, O., Leisner, T., Müller, L., Reinnig, M.-C., Hoffmann, T., Salo, K., Hallquist, M., Frosch, M., Bilde, M., Tritscher, T., Barmet, P., Praplan, A. P., DeCarlo, P. F., Dommen, J., Prévôt, A. S. H., and Baltensperger, U.: Aging of biogenic secondary organic aerosol via gas-phase OH radical reactions, P. Natl. Acad. Sci., 109, 13503–13508, doi:10.1073/pnas.1115186109, 2012b.

Draxler, R., Stunder, B., Rolph, G., Stein, A., and Taylor, A.: HYSPLIT4 User's Guide, NOAA Silver Spring, MD, 231, 2009.

Ervens, B., Turpin, B. J., and Weber, R. J.: Secondary organic aerosol formation in cloud droplets and aqueous particles (aqSOA): a review of laboratory, field and model studies, Atmos. Chem. Phys., 11, 11069–11102, doi:10.5194/acp-11-11069-2011, 2011.

Farina, S. C., Adams, P. J., and Pandis, S. N.: Modeling global secondary organic aerosol formation and processing with the volatility basis set: Implications for anthropogenic secondary organic aerosol, J. Geophys. Res. Atmos., 115, D09202, doi:10.1029/2009jd013046, 2010.

Fountoukis, C., Racherla, P. N., Denier van der Gon, H. A. C., Polymeneas, P., Charalampidis, P. E., Pilinis, C., Wiedensohler, A., Dall'Osto, M., O'Dowd, C., and Pandis, S. N.: Evaluation

of a three-dimensional chemical transport model (PMCAMx) in the European domain during the EUCAARI May 2008 campaign, Atmos. Chem. Phys., 11, 10331–10347, doi:10.5194/acp-11-10331-2011, 2011.

Fuzzi, S., Andreae, M. O., Huebert, B. J., Kulmala, M., Bond, T. C., Boy, M., Doherty, S. J., Guenther, A., Kanakidou, M., Kawamura, K., Kerminen, V.-M., Lohmann, U., Russel, L. M., and Poschl, U.: Critical assessment of the current state of scientific knowledge, terminology, and research needs concerning the role of organic aerosols in the atmosphere, climate, and global change, Atmos. Chem. Phys., 6, 2017–2038, doi:10.5194/acp-6-2017-2006, 2006.

Geever, M., O'Dowd, C. D., Ekeren, S., Flanagan, R., Nilsson, E. D., Leeuw, G., and Rannik, U.: Submicron sea spray fluxes, Geophys. Res. Lett., 32, L15810, doi:10.1029/2005GL023081, 2005.

Gelencser, A., May, B., Simpson, D., Sanchez-Ochoa, A., Kasper-Giebl, A., Puxbaum, H., Caseiro, A., Pio, C., and Legrand, M.: Source apportionment of $PM_{2.5}$ organic aerosol over Europe: Primary/secondary, natural/anthropogenic, and fossil/biogenic origin, J. Geophys. Res. Atmos., 112, D23S04, doi:10.1029/2006jd008094, 2007.

Gilardoni, S., Vignati, E., Cavalli, F., Putaud, J. P., Larsen, B. R., Karl, M., Stenström, K., Genberg, J., Henne, S., and Dentener, F.: Better constraints on sources of carbonaceous aerosols using a combined ^{14}C – macro tracer analysis in a European rural background site, Atmos. Chem. Phys., 11, 5685–5700, doi:10.5194/acp-11-5685-2011, 2011.

Goldstein, A. H. and Galbally, I. E.: Known and unexplored organic constituents in the Earth's atmosphere, Environ. Sci. Technol., 41, 1514–1521, doi:10.1021/es072476p, 2007.

Grieshop, A. P., Logue, J. M., Donahue, N. M., and Robinson, A. L.: Laboratory investigation of photochemical oxidation of organic aerosol from wood fires 1: measurement and simulation of organic aerosol evolution, Atmos. Chem. Phys., 9, 1263–1277, doi:10.5194/acp-9-1263-2009, 2009.

Griffin, R. J., Cocker III, D. R., Flagan, R. C., and Seinfeld, J. H.: Organic aerosol formation from the oxidation of biogenic hydrocarbons, J. Geophys. Res., 104, 3555–3567, 1999.

Griffin, R. J., Dabdub, D., and Seinfeld, J. H.: Secondary organic aerosol – 1. Atmospheric chemical mechanism for production of molecular constituents, J. Geophys. Res. Atmos., 107, 4332, doi:10.1029/2001jd000541, 2002.

Grosjean, D. and Seinfeld, J. H.: Parameterization of the formation potential of secondary organic aerosols, Atmos. Environ., 23, 1733–1747, doi:10.1016/0004-6981(89)90058-9, 1989.

Guenther, A., Karl, T., Harley, P., Wiedinmyer, C., Palmer, P. I., and Geron, C.: Estimates of global terrestrial isoprene emissions using MEGAN (Model of Emissions of Gases and Aerosols from Nature), Atmos. Chem. Phys., 6, 3181–3210, doi:10.5194/acp-6-3181-2006, 2006.

Hallquist, M., Wenger, J. C., Baltensperger, U., Rudich, Y., Simpson, D., Claeys, M., Dommen, J., Donahue, N. M., George, C., Goldstein, A. H., Hamilton, J. F., Herrmann, H., Hoffmann, T., Iinuma, Y., Jang, M., Jenkin, M. E., Jimenez, J. L., Kiendler-Scharr, A., Maenhaut, W., McFiggans, G., Mentel, Th. F., Monod, A., Prévôt, A. S. H., Seinfeld, J. H., Surratt, J. D., Szmigielski, R., and Wildt, J.: The formation, properties and impact of secondary organic aerosol: current and emerging issues, Atmos. Chem. Phys., 9, 5155–5236, doi:10.5194/acp-9-5155-

2009, 2009.

Hildebrandt, L., Engelhart, G. J., Mohr, C., Kostenidou, E., Lanz, V. A., Bougiatioti, A., DeCarlo, P. F., Prevot, A. S. H., Baltensperger, U., Mihalopoulos, N., Donahue, N. M., and Pandis, S. N.: Aged organic aerosol in the Eastern Mediterranean: the Finokalia Aerosol Measurement Experiment-2008, Atmos. Chem. Phys., 10, 4167–4186, doi:10.5194/acp-10-4167-2010, 2010a.

Hildebrandt, L., Kostenidou, E., Mihalopoulos, N., Worsnop, D. R., Donahue, N. M., and Pandis, S. N.: Formation of highly oxygenated organic aerosol in the atmosphere: Insights from the Finokalia Aerosol Measurement Experiments, Geophys. Res. Lett., 37, L23801, doi:10.1029/2010gl045193, 2010b.

Hodzic, A., Jimenez, J. L., Madronich, S., Canagaratna, M. R., DeCarlo, P. F., Kleinman, L., and Fast, J.: Modeling organic aerosols in a megacity: potential contribution of semi-volatile and intermediate volatility primary organic compounds to secondary organic aerosol formation, Atmos. Chem. Phys., 10, 5491–5514, doi:10.5194/acp-10-5491-2010, 2010.

Huffman, J. A., Docherty, K. S., Mohr, C., Cubison, M. J., Ulbrich, I. M., Ziemann, P. J., Onasch, T. B., and Jimenez, J. L.: Chemically-resolved volatility measurements of organic aerosol from different sources, Environ. Sci. Technol., 43, 5351–5357, doi:10.5194/acp-9-7161-2009, 2009.

IPCC: Climate Change 2007: The physical science basis. Contribution of working group I to the fourth assessment report of the Intergovernmental Panel on Climate Change, Press, C. U. Cambridge, United Kingdom and New York, NY, USA, 996, 2007.

Isaksen, I. S. A., Granier, C., Myhre, G., Berntsen, T. K., Dalsøren, S. B., Gauss, M., Klimont, Z., Benestad, R., Bousquet, P., Collins, W., Cox, T., Eyring, V., Fowler, D., Fuzzi, S., Jöckel, P., Laj, P., Lohmann, U., Maione, M., Monks, P., Prevot, A. S. H., Raes, F., Richter, A., Rognerud, B., Schulz, M., Shindell, D., Stevenson, D. S., Storelvmo, T., Wang, W. C., van Weele, M., Wild, M., and Wuebbles, D.: Atmospheric composition change: climate-chemistry interactions, Atmos. Environ., 43, 5138–5192, 2009.

Jimenez, J. L., Canagaratna, M. R., Donahue, N. M., Prevot, A. S. H., Zhang, Q., Kroll, J. H., DeCarlo, P. F., Allan, J. D., Coe, H., Ng, N. L., Aiken, A. C., Docherty, K., Ulbrich, I., Grieshop, A. P., Robinson, A. L., Duplissy, J., Smith, J. D., Wilson, K. R., Lanz, V. A., Hueglin, C., Sun, Y. L., Tian, J., Laaksonen, A., Raatikainen, T., Rautiainen, J., Vaattovaara, P., Ehn, M., Kulmala, M., Tomlinson, J. M., Collins, D. R., Cubison, M. J., Dunlea, E., Huffman, J. A., Onasch, T. B., Alfarra, M. R., Williams, P., Bower, K., Kondo, Y., Schneider, J., Drewnick, F., Borrmann, S., Weimer, S., Demerjian, K., Salcedo, D., Cottrell, L., Griffin, R. J., Takami, A., Miyoshi, T., Hatakeyama, S., Shimono, A., Sun, J. Y., Zhang, Y. M., Dzepina, K., Kimmel, J. R., Sueper, D., Jayne, J. T., Herndon, S. C., Trimborn, A., Williams, L. R., Wood, E. C., Middlebrook, A. M., Kolb, C. E., Baltensperger, U., and Worsnop, D. R.: Evolution of organic aerosols in the atmosphere, Science, 326, 1525–1529, 2009.

Johnson, D., Utembe, S. R., Jenkin, M. E., Derwent, R. G., Hayman, G. D., Alfarra, M. R., Coe, H., and McFiggans, G.: Simulating regional scale secondary organic aerosol formation during the TORCH 2003 campaign in the southern UK, Atmos. Chem. Phys., 6, 403–418, doi:10.5194/acp-6-403-2006, 2006.

Kanakidou, M., Seinfeld, J. H., Pandis, S. N., Barnes, I., Dentener, F. J., Facchini, M. C., Van Dingenen, R., Ervens, B., Nenes, A.,

Nielsen, C. J., Swietlicki, E., Putaud, J. P., Balkanski, Y., Fuzzi, S., Horth, J., Moortgat, G. K., Winterhalter, R., Myhre, C. E. L., Tsigaridis, K., Vignati, E., Stephanou, E. G., and Wilson, J.: Organic aerosol and global climate modelling: a review, Atmos. Chem. Phys., 5, 1053–1123, doi:10.5194/acp-5-1053-2005, 2005.

Kostenidou, E., Lee, B. H., Engelhart, G. J., Pierce, J. R., and Pandis, S. N.: Mass spectra deconvolution of low, medium, and high volatility biogenic secondary organic aerosol, Environ. Sci. Technol., 43, 4884–4889, doi:10.1021/Es803676g, 2009.

Kroll, J. H. and Seinfeld, J. H.: Chemistry of secondary organic aerosol: Formation and evolution of low-volatility organics in the atmosphere, Atmos. Environ., 42, 3593–3624, doi:10.1016/j.atmosenv.2008.01.003, 2008.

Kroll, J. H., Smith, J. D., Che, D. L., Kessler, S. H., Worsnop, D. R., and Wilson, K. R.: Measurement of fragmentation and functionalization pathways in the heterogeneous oxidation of oxidized organic aerosol, Phys. Chem. Chem. Phys., 11, 8005–8014, doi:10.1039/B905289e, 2009.

Kroll, J. H., Donahue, N. M., Jimenez, J. L., Kessler, S. H., Canagaratna, M. R., Wilson, K. R., Altieri, K. E., Mazzoleni, L. R., Wozniak, A. S., Bluhm, H., Mysak, E. R., Smith, J. D., Kolb, C. E., and Worsnop, D. R.: Carbon oxidation state as a metric for describing the chemistry of atmospheric organic aerosol, Nat. Chem., 3, 133–139, doi:10.1038/Nchem.948, 2011.

Kulmala, M., Asmil, A., Lappalainen, H. K., Carslaw, K. S., Poschl, U., Baltensperger, U., Hoy, O., Brenquier, J.-L., Pandis, S. N., Facchini, M. C., Hansson, H. C., Wiedensohler, A., and O'Dowd, C. D.: Introduction: European Integrated Project on Aerosol Cloud Climate and Air Quality interactions (EUCAARI) – integrating aerosol research from nano to global scales, Atmos. Chem. Phys., 9, 2825–2841, doi:10.5194/acp-9-2825-2009, 2009.

Kulmala, M., Asmi, A., Lappalainen, H. K., Baltensperger, U., Brenguier, J.-L., Facchini, M. C., Hansson, H.-C., Hov, Ø., O'Dowd, C. D., Pöschl, U., Wiedensohler, A., Boers, R., Boucher, O., de Leeuw, G., Denier van der Gon, H. A. C., Feichter, J., Krejci, R., Laj, P., Lihavainen, H., Lohmann, U., McFiggans, G., Mentel, T., Pilinis, C., Riipinen, I., Schulz, M., Stohl, A., Swietlicki, E., Vignati, E., Alves, C., Amann, M., Ammann, M., Arabas, S., Artaxo, P., Baars, H., Beddows, D. C. S., Bergström, R., Beukes, J. P., Bilde, M., Burkhart, J. F., Canonaco, F., Clegg, S. L., Coe, H., Crumeyrolle, S., D'Anna, B., Decesari, S., Gilardoni, S., Fischer, M., Fjaeraa, A. M., Fountoukis, C., George, C., Gomes, L., Halloran, P., Hamburger, T., Harrison, R. M., Herrmann, H., Hoffmann, T., Hoose, C., Hu, M., Hyvärinen, A., Hõrrak, U., Iinuma, Y., Iversen, T., Josipovic, M., Kanakidou, M., Kiendler-Scharr, A., Kirkevåg, A., Kiss, G., Klimont, Z., Kolmonen, P., Komppula, M., Kristjánsson, J.-E., Laakso, L., Laaksonen, A., Labonnote, L., Lanz, V. A., Lehtinen, K. E. J., Rizzo, L. V., Makkonen, R., Manninen, H. E., McMeeking, G., Merikanto, J., Minikin, A., Mirme, S., Morgan, W. T., Nemitz, E., O'Donnell, D., Panwar, T. S., Pawlowska, H., Petzold, A., Pienaar, J. J., Pio, C., Plass-Duelmer, C., Prévôt, A. S. H., Pryor, S., Reddington, C. L., Roberts, G., Rosenfeld, D., Schwarz, J., Seland, Ø., Sellegri, K., Shen, X. J., Shiraiwa, M., Siebert, H., Sierau, B., Simpson, D., Sun, J. Y., Topping, D., Tunved, P., Vaattovaara, P., Vakkari, V., Veefkind, J. P., Visschedijk, A., Vuollekoski, H., Vuolo, R., Wehner, B., Wildt, J.,

Woodward, S., Worsnop, D. R., van Zadelhoff, G.-J., Zardini, A. A., Zhang, K., van Zyl, P. G., Kerminen, V.-M., S Carslaw, K., and Pandis, S. N.: General overview: European Integrated project on Aerosol Cloud Climate and Air Quality interactions (EUCAARI) – integrating aerosol research from nano to global scales, Atmos. Chem. Phys., 11, 13061–13143, doi:10.5194/acp-11-13061-2011, 2011.

Lane, T. E., Donahue, N. M., and Pandis, S. N.: Simulating secondary organic aerosol formation using the volatility basis-set approach in a chemical transport model, Atmos. Environ., 42, 7439–7451, doi:10.1016/j.atmosenv.2008.06.026, 2008.

Lee, B.-H., Pierce, J. R., Engelhart, G. J., and Pandis, S. N.: Volatility of secondary organic aerosol from the ozonolysis of monoterpenes, Atmos. Environ., 45, 2443–2452, 2011.

Mensah, A. A., Holzinger, R., Otjes, R., Trimborn, A., Mentel, Th. F., ten Brink, H., Henzing, B., and Kiendler-Scharr, A.: Aerosol chemical composition at Cabauw, The Netherlands as observed in two intensive periods in May 2008 and March 2009, Atmos. Chem. Phys., 12, 4723–4742, doi:10.5194/acp-12-4723-2012, 2012.

Morgan, W. T., Allan, J. D., Bower, K. N., Esselborn, M., Harris, B., Henzing, J. S., Highwood, E. J., Kiendler-Scharr, A., McMeeking, G. R., Mensah, A. A., Northway, M. J., Osborne, S., Williams, P. I., Krejci, R., and Coe, H.: Enhancement of the aerosol direct radiative effect by semi-volatile aerosol components: airborne measurements in North-Western Europe, Atmos. Chem. Phys., 10, 8151–8171, doi:10.5194/acp-10-8151-2010, 2010a.

Morgan, W. T., Allan, J. D., Bower, K. N., Highwood, E. J., Liu, D., McMeeking, G. R., Northway, M. J., Williams, P. I., Krejci, R., and Coe, H.: Airborne measurements of the spatial distribution of aerosol chemical composition across Europe and evolution of the organic fraction, Atmos. Chem. Phys., 10, 4065–4083, doi:10.5194/acp-10-4065-2010, 2010b.

Murphy, B. N. and Pandis, S. N.: Simulating the formation of semivolatile primary and secondary organic aerosol in a regional chemical transport model, Environ. Sci. Technol., 43, 4722–4728, doi:10.1021/Es803168a, 2009.

Murphy, B. N. and Pandis, S. N.: Exploring summertime organic aerosol formation in the eastern United States using a regional-scale budget approach and ambient measurements, J. Geophys. Res., 115, D24216, doi:10.1029/2010JD014418, 2010.

Murphy, B. N., Donahue, N. M., Fountoukis, C., and Pandis, S. N.: Simulating the oxygen content of ambient organic aerosol with the 2D volatility basis set, Atmos. Chem. Phys., 11, 7859–7873, doi:10.5194/acp-11-7859-2011, 2011.

Myriokefalitakis, S., Tsigaridis, K., Mihalopoulos, N., Sciare, J., Nenes, A., Kawamura, K., Segers, A., and Kanakidou, M.: In-cloud oxalate formation in the global troposphere: a 3-D modeling study, Atmos. Chem. Phys., 11, 5761–5782, doi:10.5194/acp-11-5761-2011, 2011.

Ng, N. L., Kroll, J. H., Keywood, M. D., Bahreini, R., Varutbangkul, V., Flagan, R. C., and Seinfeld, J. H.: Contribution of first- versus second-generation products to secondary organic aerosols formed in the oxidation of biogenic hydrocarbons, Environ. Sci. Technol., 40, 2283–2297, 2006.

Ng, N. L., Canagaratna, M. R., Zhang, Q., Jimenez, J. L., Tian, J., Ulbrich, I., Kroll, J. H., Docherty, K., Chhabra, P. S., Bahreini, R., Murphy, S. M., Seinfeld, J. H., Hildebrandt, L., DeCarlo,

P. F., Lanz, V. A., Prevot, A. S. H., Dinar, E., Rudlich, Y., and Worsnop, D. R.: Organic aerosol components observed in Northern Hemispheric datasets from aerosol mass spectrometry, Atmos. Chem. Phys., 10, 4625–4641, doi:10.5194/acp-10-4625-2010, 2010.

O'Dowd, C. D., Langmann, B., Varghese, S., Scannell, C., Ceburnis, D., and Facchini, M. C.: A combined organic-inorganic sea spray source function, Geophys. Res. Lett., 35, L01801, doi:10.1029/2007GL030331, 2008.

Odum, J. R., Jungkamp, T. P. W., Griffin, R. J., Forstner, H. J. L., Flagan, R. C., and Seinfeld, J. H.: Aromatics, reformulated gasoline, and atmospheric organic aerosol formation, Environ. Sci. Technol., 31, 1890–1897, 1997.

Pandis, S. N., Harley, R. A., Cass, G. R., and Seinfeld, J. H.: Secondary organic aerosol formation and transport, Atmos. Environ. A-Gen., 26, 2269–2282, 1992.

Pandis, S. N., Wexler, A. S., and Seinfeld, J. H.: Dynamics of tropospheric aerosols, The Journal of Physical Chemistry, 99, 9646–9659, doi:10.1021/j100024a003, 1995.

Pankow, J. F. and Asher, W. E.: SIMPOL.1: a simple group contribution method for predicting vapor pressures and enthalpies of vaporization of multifunctional organic compounds, Atmos. Chem. Phys., 8, 2773–2796, doi:10.5194/acp-8-2773-2008, 2008.

Pankow, J. F. and Barsanti, K. C.: The carbon number-polarity grid: A means to manage the complexity of the mix of organic compounds when modeling atmospheric organic particulate matter, Atmos. Environ., 43, 2829–2835, 2009.

Pikridas, M., Bougiatioti, A., Hildebrandt, L., Engelhart, G. J., Kostenidou, E., Mohr, C., Prevot, A. S. H., Kouvarakis, G., Zarmpas, P., Burkhart, J. F., Lee, B.-H., Psichoudaki, M., Mihalopoulos, N., Pilinis, C., Stohl, A., Baltensperger, U., Kulmala, M., and Pandis, S. N.: The Finokalia Aerosol Measurement Experiment – 2008 (FAME-08): an overview, Atmos. Chem. Phys., 10, 6793–6806, doi:10.5194/acp-10-6793-2010, 2010.

Pope, C. A., Ezzati, M., and Dockery, D. W.: Fine-particulate air pollution and life expectancy in the United States, New England Journal of Medicine, 360, 376–386, doi:10.1056/NEJMsa0805646, 2009.

Pun, B. K., Griffin, R. J., Seigneur, C., and Seinfeld, J. H.: Secondary organic aerosol – 2. Thermodynamic model for gas/particle partitioning of molecular constituents, J. Geophys. Res. Atmos., 107, 4333 doi:10.1029/2001jd000542, 2002.

Qi, L., Nakao, S., Malloy, Q., Warren, B., and Cocker, D. R.: Can secondary organic aerosol formed in an atmospheric simulation chamber continuously age?, Atmos. Environ., 44, 2990–2996, doi:10.1016/j.atmosenv.2010.05.020, 2010.

Robinson, A. L., Donahue, N. M., Shrivastava, M. K., Weitkamp, E. A., Sage, A. M., Grieshop, A. P., Lane, T. E., Pierce, J. R., and Pandis, S. N.: Rethinking organic aerosols: Semivolatile emissions and photochemical aging, Science, 315, 1259–1262, doi:10.1126/science.1133061, 2007.

Rudich, Y., Donahue, N. M., and Mentel, T. F.: Aging of organic aerosol: bridging the gap between laboratory and field studies, Annu. Rev. Phys. Chem., 58, 321–352, doi:10.1146/annurev.physchem.58.032806.104432, 2007.

Sareen, N., Schwier, A. N., Shapiro, E. L., Mitroo, D., and McNeill, V. F.: Secondary organic material formed by methylglyoxal in aqueous aerosol mimics, Atmos. Chem. Phys., 10, 997–1016,

doi:10.5194/acp-10-997-2010, 2010.

Seinfeld, J. H. and Pandis, S. N.: Atmospheric Chemistry and Physics: From Air Pollution to Climate Change, 2nd Ed., John Wiley and Sons, Hoboken, New Jersey, 2006.

Shilling, J. E., Chen, Q., King, S. M., Rosenoern, T., Kroll, J. H., Worsnop, D. R., DeCarlo, P. F., Aiken, A. C., Sueper, D., Jimenez, J. L., and Martin, S. T.: Loading-dependent elemental composition of α-pinene SOA particles, Atmos. Chem. Phys., 9, 771–782, doi:10.5194/acp-9-771-2009, 2009.

Shrivastava, M. K., Lane, T. E., Donahue, N. M., Pandis, S. N., and Robinson, A. L.: Effects of gas particle partitioning and aging of primary emissions on urban and regional organic aerosol concentrations, J. Geophys. Res. Atmos., 113, D18301, doi:10.1029/2007jd009735, 2008.

Simpson, D., Yttri, K. E., Klimont, Z., Kupiainen, K., Caseiro, A., Gelencsér, A., Pio, C., Puxbaum, H., and Legrand, M.: Modeling carbonaceous aerosol over Europe: Analysis of the CARBOSOL and EMEP EC/OC campaigns, J. Geophys. Res., 112, D23S14, doi:10.1029/2006jd008158, 2007.

Skamarock, W. C., Klemp, J. B., Dudhia, J., Gill, D. O., Duda, M. G., Huang, X., Wang, W., and Powers, J. G.: A description of the advanced research WRF version 3, National Center for Atmspheric Research (NCAR) Boulder, CONCAR/TN-475+STR, 2008.

Sofiev, M., Lanne, M., Vankevich, R., Prank, M., Karppinen, A., and Kukkonen, J.: Impact of wild-land fires on European air quality in 2006–2008, Modeling, Monitoring and Management of Forest Fires, WIT Trans. on Ecology and the Environment, 119, 353–361, 2008a.

Sofiev, M., Vankevich, R., Lanne, M., Koskinen, J., and Kukkonen, J.: On integration of a Fire Assimilation System and a chemical transport model for near-real-time monitoring of the impact of wild-land fires on atmospheric composition and air quality, Modeling, Monitoring and Management of Forest Fires, WIT Trans. on Ecology and the Environment, 119, 343–351, 2008b.

Stanier, C. O., Pathak, R. K., and Pandis, S. N.: Measurements of the volatility of aerosols from α-pinene ozonolysis, Environ. Sci. Technol., 41, 2756–2763, doi:10.1021/es0519280, 2007.

Szidat, S., Jenk, T. M., Synal, H.-A., Kalberer, M., Wacker, L., Hajdas, I., Kasper-Giebl, A., and Baltensperger, U.: Contributions of fossil fuel, biomass-burning, and biogenic emissions to carbonaceous aerosols in Zurich as traced by 14C, J. Geophys. Res., 111, D07206, doi:10.1029/2005jd006590, 2006.

Tritscher, T., Dommen, J., DeCarlo, P. F., Gysel, M., Barmet, P. B., Praplan, A. P., Weingartner, E., Prévôt, A. S. H., Riipinen, I., Donahue, N. M., and Baltensperger, U.: Volatility and hygroscopicity of aging secondary organic aerosol in a smog chamber, Atmos. Chem. Phys., 11, 11477–11496, doi:10.5194/acp-11-11477-2011, 2011.

Tsimpidi, A. P., Karydis, V. A., Zavala, M., Lei, W., Molina, L., Ulbrich, I. M., Jimenez, J. L., and Pandis, S. N.: Evaluation of the volatility basis-set approach for the simulation of organic aerosol formation in the Mexico City metropolitan area, Atmos. Chem. Phys., 10, 525–546, doi:10.5194/acp-10-525-2010, 2010.

Vaden, T. D., Imre, D., Beránek, J., Shrivastava, M., and Zelenyuk, A.: Evaporation kinetics and phase of laboratory and ambient secondary organic aerosol, P. Natl. Acad. Sci., 108, 2190–2195, 2011.

Visschedijk, A. J., Zandveld, P., and Denier van der Gon, H. A. C.: TNO Report 2007 A-R0233/B: A high resolution gridded European emission database for the EU integrated project GEMS, Organization for Applied Scientific Research Netherlands, 2007.

Washenfelder, R. A., Young, C. J., Brown, S. S., Angevine, W. M., Atlas, E. L., Blake, D. R., Bon, D. M., Cubison, M. J., de Gouw, J. A., Dusanter, S., Flynn, J., Gilman, J. B., Graus, M., Griffith, S., Grossberg, N., Hayes, P. L., Jimenez, J. L., Kuster, W. C., Lefer, B. L., Pollack, I. B., Ryerson, T. B., Stark, H., Stevens, P. S., and Trainer, M. K.: The glyoxal budget and its contribution to organic aerosol for Los Angeles, California, during CalNex 2010, J. Geophys. Res., 116, D00V02, doi:10.1029/2011jd016314, 2011.

Weitkamp, E. A., Lambe, A. T., Donahue, N. M., and Robinson, A. L.: Laboratory measurements of the heterogeneous oxidation of condensed-phase organic molecular makers for motor vehicle exhaust, Environ. Sci. Technol., 42, 7950–7956, doi:10.1021/es800745x, 2008.

Yttri, K. E., Simpson, D., Nøjgaard, J. K., Kristensen, K., Genberg, J., Stenström, K., Swietlicki, E., Hillamo, R., Aurela, M., Bauer, H., Offenberg, J. H., Jaoui, M., Dye, C., Eckhardt, S., Burkhart, J. F., Stohl, A., and Glasius, M.: Source apportionment of the summer time carbonaceous aerosol at Nordic rural background sites, Atmos. Chem. Phys., 11, 13339–13357, doi:10.5194/acp-11-13339-2011, 2011.

Zhang, Q., Jimenez, J. L., Canagaratna, M. R., Allan, J. D., Coe, H., Ulbrich, I., Alfarra, M. R., Takami, A., Middlebrook, A. M., Sun, Y. L., Dzepina, K., Dunlea, E., Docherty, K., DeCarlo, P. F., Salcedo, D., Onasch, T., Jayne, J. T., Miyoshi, T., Shimono, A., Hatakeyama, S., Takegawa, N., Kondo, Y., Schneider, J., Drewnick, F., Borrmann, S., Weimer, S., Demerjian, K., Williams, P., Bower, K., Bahreini, R., Cottrell, L., Griffin, R. J., Rautiainen, J., Sun, J. Y., Zhang, Y. M., and Worsnop, D. R.: Ubiquity and dominance of oxygenated species in organic aerosols in anthropogenically-influenced Northern Hemisphere midlatitudes, Geophys. Res. Lett., 34, L13801–13806, doi:10.1029/2007GL029979, 2007.